A thesis submitted in partial fulfilment for the degree of
Master of Science in Forest Sciences and Forest Ecology

Land Cover Classification for Jambi Province, Indonesia using two different remote sensing techniques: visual interpretation and supervised classification

RODRIGO PAUL VERA RAMIREZ

Faculty of Forest Sciences and Forest Ecology
GEORG-AUGUST-UNIVERSITÄT GÖTTINGEN
Göttingen, Germany

Submitted on December 20th, 2018

Land Cover Classification for Jambi Province, Indonesia using two remote sensing techniques: visual interpretation and supervised classification

RODRIGO PAUL VERA RAMIREZ

r.veraramirez@stud.uni-goettingen.de

Supervisors:

1. Mrs. Kira Urban, MSc

Chair of Forest Inventory and Remote Sensing, Faculty of Forest Sciences and Forest Ecology, Georg-August-University Göttingen, Germany

2. Prof Dr Ir I Nengah Surati Jaya, MAgr

Forest Resources Inventory, Remote Sensing & GIS Laboratories, Faculty of Forestry, Bogor Agricultural University, Indonesia

Master Thesis 2018

Faculty of Forest Sciences and Forest Ecology

Georg-August-University Göttingen

Acknowledgements

Rodrigo Vera

ABSTRACT

Land Cover (LC) maps are one of the most important topics in remote sensing. Their interpretation and changes are critical in the planning and management of natural resources in a specific region. These maps are generated using digital image interpretation. One of the main challenges with this process is the presence of clouds and haze. The purposes of this study were to perform and evaluate two image interpretation techniques for LC classification in Jambi province, Indonesia, and to find the best pathway to obtain a high-quality updated LC map.

For the first technique, visual interpretation, a grid of 1009 plots, systematically distributed, was overlaid in the whole province boundary layer. Therefore, each plot was labeled with an LC class using a set of multi-temporal imagery. For the second technique, supervised classification, a Landsat-8 satellite image mosaic was generated to cover the study area. The mosaic was pre-processed and enhanced before the classification phase. Reference data, that were gathered from the field, were divided into two groups, i.e., for training data set and for accuracy assessment on validation phase. In this study, the classified image of 2013 was used to compare the results.

Results from both techniques were different from each other for several LC classes. Some unexpected results in LC classification were found when comparing with the 2013 classification. These results could have occurred because of: user's skills for visual interpretation technique, similarities between different LC classes, old digital image sources that did not fit with the Landsat-8 image mosaic, large cloud cover in the mosaic, and heterogeneous classification keys between the two techniques.

In conclusion, to generate an accurate quality updated LC map, both techniques should be complementarily used. Classified plots from visual interpretation (using 2018 imagery) should be mixed with fieldwork reference data, and additionally, a more complex compositing technique with 2018 imagery should be executed for a cloud-free Landsat-8 satellite image mosaic.

Keywords: Digital image interpretation, LC classification, visual interpretation, supervised classification, cloud cover, Jambi province.

ZUSAMMENFASSUNG

Landbedeckungskartierungen (engl. Land Cover (LC) maps) sind eines der wichtigsten Themen der Fernerkundung. Ihre Interpretation und Veränderungen sind für die Planung und das Management natürlicher Ressourcen in einer bestimmten Region von entscheidender Bedeutung. Diese Karten werden mit digitaler Bildinterpretation erstellt. Eine der größten Herausforderungen bei diesem Prozess sind vorhandene Wolken und Dunst. Das Ziel dieser Studie war es, zwei Bildinterpretationstechniken für die LC-Klassifizierung für die Provinz Jambi, Indonesien, durchzuführen und den besten Weg zu finden, um mit ihnen eine aktualisierte LC-Karte von hoher Qualität zu erhalten.

Zur visuellen Interpretation wurde in der gesamten Provinz ein systematisch verteiltes Netz von 1009 Parzellen überlagert. Folglich wurde jede Darstellung mit einer LC-Klasse unter Verwendung eines Satzes von multitemporalen Bildern markiert. Für die überwachte Klassifizierung wurde ein Landsat-8-Satellitenbildmosaik der gesamten Provinz erstellt und vor der Klassifizierungsphase bearbeitet und verbessert. Referenzdaten wurden aus dem Feld gesammelt und in zwei Gruppen für die Schulungs- und Validierungsphase aufgeteilt. Für diese Daten wurde ein überwachter Klassifizierungsalgorithmus durchgeführt. Die Klassifizierung von 2013 wurde verwendet, um die Ergebnisse zu vergleichen.

Die Ergebnisse beider Techniken unterschieden sich für mehrere LC-Klassen. Beim Vergleich mit der Klassifizierung von 2013 wurden einige unerwartete Ergebnis der LC-Bereiche gefunden. Diese Ergebnisse könnten folgende Ursachen haben: Fähigkeiten des Anwenders für die visuelle Interpretationstechnik, Ähnlichkeiten zwischen verschiedenen LC-Klassen, alte digitale Bildquellen, die nicht zum Landsat-8-Bildmosaik passen, großflächige Wolkenbedeckung im Mosaik und heterogene Klassifizierungsschlüssel zwischen den beiden Techniken.

Um genaue aktualisierte LC-Karten zu erstellen, sollten beide Techniken ergänzend eingesetzt werden. Klassifizierte Diagramme aus visueller Interpretation (unter Verwendung von 2018-Bildern) sollten mit Feldreferenzdaten gemischt werden, und eine Kompositions-Technik mit 2018-Bildern für ein wolkenfreies Landsat-8-Satellitenbildmosaik ausgeführt werden sollte.

RINGKASAN

Peta Tutupan Lahan (Tuplah) adalah salah satu topik yang sangat penting dalam penginderaan jauh. Interpretasi dan analisis perubahan dari suatu tutupan lahan sangat penting manfaatnya dalam perencanaan dan pengelolaan sumber daya alam di wilayah tertentu. Tuplah-tuplah ini pada umumnya dihasilkan dari klasifikasi citra digital. Akan tetapi, salah satu tantangan utama dalam pengolahan citra disini adalah keberadaan awan dan kabut. Tujuan utama dari penelitian ini adalah untuk menguji keterhandalan dua teknik interpretasi citra guna menghasilkan Tuplah di Provinsi Jambi, Indonesia, sekaligus untuk menemukan metode terbaik untuk menghasilkan Tuplah terbaru yang akurat. Untuk metode interpretasi visual, tehnik interpretasinya menggunakan grid sebanyak 1009 plot, yang tersebar secara sistematis, ditumpangtindihkan dengan batas wilayah seluruh Provinsi Jambi. Lebih lanjut, setiap plot diberi label nama salah satu dari tutupan lahan yang telah didefinisikan sebelumnya menggunakan serangkaian citra multi-waktu. Pada metode klasifikasi terbimbing, dibuat mosaic citra Landsat-8 untuk seluruh Provinsi Jambi yang diperoleh dari proses mosaic dan penajaman citra sebelum dilakukan klasifikasi. Data referensi dikumpulkan dari lapangan dan dibagi menjadi dua kelompok yaitu untuk data latih (*training area)* pada tahap pengolahan dan data pengujian akurasi pada tahap validasi. Pada kajian ini, hasil klasifikasi tahun 2013 digunakan sebagai membandingkan hasil.

Hasil kajian dari kedua teknik itu memperlihatkan perbedaan satu sama lain, khususnya untuk beberapa kelas tutupan lahan. Beberapa hasil yang tidak diharapkan dalam klasifikasi tutupan lahan ditemukan ketika membandingkannya dengan hasil klasifikasi 2013. Hasil dari interpretasi visual ini dapat terjadi karena: keterampilan dari analis (interpreter) dalam melakukan teknik interpretasi visual, kesamaan antara kelas tutupan lahan yang berbeda, kualitas sumber citra digital dari waktu sebelumnya tidak sesuai dengan mosaik citra Landsat-8 yang digunakan saat analisis, tutupan awan yang cukup banyak pada citra hasil mosaik, dan kunci kelas-kelas yang cukup beragam dari dua tehnik yang diterapkan. Kesimpulannya, untuk menghasilkan tuplah terbaru dengan kualitas yang akurat, kedua teknik harus digunakan secara bergantian dan saling melengkapi (komplementer). Plot yang diklasifikasi dengan tehnik interpretasi visual menggunakan citra tahun 2018) harus digabungkan dengan hasil data rujukan lapangan dan data dari sumber lain. Teknik membuat citra komposit 2018 sebaiknya dilakukan menggunakan mosaik citra satelit Landsat-8 yang bebas awan.

Contents

List of figures

List of tables

List of abbreviations

AoI	Area of Interest
ASTER	Advanced Spaceborne Thermal Emission and Reflection Radiometer
BAP	Based-Available-Pixel
CNES	Centre National d'Études Spatiales
CRC	Collaborative Research Centre
DN	Digital Number
EFForTS	Ecological and Socioeconomic Functions of Tropical Lowland Rainforest Transformation Systems (Sumatra, Indonesia)
EOS	Earth Observing System
FAO	Food and Alimentation Organization
GB	Gigabytes
GEE	Google Earth Engine
GIS	Geographic Information System
GPS	Global Positioning System
IDE	Integrated Development Editor
IPCC	Intergovernmental Panel on Climate Change
km	Kilometre
km2	squared kilometre
LC	Land Cover
LU	Land Use
m	meter
mm	millimetre
m a.s.l.	meters above sea level
MODIS	Moderate Resolution Imaging Spectroradiometer
n	number
NASA	National Aeronautics and Space Administration
NDVI	Normalized Density Vegetation Index
NIR	Near-infra red
OA	Overall Assessment
OF-CE	Open Foris - Collect Earth

OTB	Orfeo Toolbox
P	Path
p	proportion
PA	Producer Assessment
PAN	Panchromatic
PCA	Principal Component Analysis
QGIS	Quantum GIS
R	Row
RF	Random Forest
RGB	Red-Green-Blue
ROI	Regions of Interest
SCP	Semi-Automatic Classification Plugin
SE	Standard Error
SWIR	Short-Wavelength Infrared
TIRS	Thermal Infrared Sensor
TOF	Trees Outside the Forest
UA	User Assessment
UNFCCC	United Nations Framework Convention for Climate Change
USGS	United States Geological Survey
VIS	Visible Infrared
WGS	World Geodetic System
µm	micrometre

1. Introduction

1.1 Definitions and background

The definition and differentiation between land cover (LC) and land use (LU) map are critical, thus, finding confusions between these two terms is common (Di Gregorio and Jansen 2000). LC can be defined as "an observed (bio) physical cover on earth's surface" (Di Gregorio and Jansen 2000). Therefore, LC indicates how much forest, wetlands, agriculture, untouched areas, water bodies, among others, are covered in a determined region (US Department of Commerce 2017). LC maps are used for generating approximations associated with earth surface dynamics over time. (Di Gregorio 2016).

On the other hand, LU is a term related to the arrangements, inputs, and activities that people implement in certain land cover types. LU definition could be explained as the link between land cover and human activities affecting its environment (Di Gregorio and Jansen 2000). Another definition states that LU is the purpose or aim which an LC is supposed to have. For instance, if the LC is a forest or woodland, the LU would be timber production, forest conservation, among others (Australian Department of Agriculture and Water Resources 2017). Identification of LU classes is needed for suggesting the best use for lands. (Golmehr 2009).

In respect of the interests of this study, the main difference between both definitions is that the LC of a determined region can be assessed using satellite imagery, unlike LU (US Department of Commerce 2017). Moreover, LU requires a broader knowledge over the Area of Interest (AoI). Many studies use both concepts together: when LUs are the variable of interest, LC is used as a tool to identify them (Fonji and Taff 2014).

Due to the importance of the LC maps in remote sensing, their knowledge and changes are crucial to plan and manage the natural resources in a particular area (Lam 2008). LC maps are not only a valuable source of information, but also the base of analysis for decision making in different fields, such as forestry, conservation, fire control & detection, LC changes, among others (Bontemps et al. 2013).

The LC results produced in this study are to be used under the framework of the project "Collaborative Research Centre 990 (CRC): Ecological and Socioeconomic Functions of Tropical Lowland Rainforest Transformation Systems (Sumatra, Indonesia) (EFForTS)".

1.2. Challenges of image classification using digital imagery in Indonesia

Some of the most relevant challenges in Indonesia are land and forest fire events. These events have been relatively high since 1982/1983, when 36 000 km^2 of the tropical rainforest of Kalimantan were burned out. Consequently, several fire events have been recurrent through time and connected to extreme weather events (Syaufina, Sitanggang, and Erman 2016). An extreme case occurred in 2015, when 26 110 km^2 of land were burned between June and October (The World Bank 2016). Haze production with particulate emissions is the principal impact of forest and land fires (Heriyanto, Syaufina, and Sobri 2015).

Therefore, the challenge for imagery interpretation turns into cloud cover and haze: Cloud cover is the main source for solar radiation blockage (Escrig et al. 2013). Moreover, cloud cover could be so thick that the land below cannot be identified, whereas, in some haze areas, information can also be unrecognizable or altered (Xiangsheng, Yonggang, and Anding 2011). A different LC could look the same when observed from the same satellite (Fonji and Taff 2014).

Even though a relatively small monthly free-cloud cover window could be defined for particular areas in Indonesia in the past years (Gastellu-Etchegorry 1988), currently, a seasonally cloud-free window is unavailable. Therefore more data is required to overlay cloud patches on an imagery mosaic (Arunarwati Margono et al. 2012). Hence, the need for seasonally cloud-free imagery is increasing (Dewanti Dimyati et al. 2018).

1.3. Digital image interpretation approaches

Two approaches are described for image interpretation on remote sensing (Richards 2013). The first one: photo interpretation, is connected to the cognitive ability of the user, local knowledge and experience. Meanwhile, the second one: quantitative analysis, uses statistics algorithms for detection of patterns. Both approaches have several differences

but could work complementarily on digital image interpretation. Their characteristics are described in Table 1:

Table 1 Characteristics two approaches for LC classification: photointerpretation and quantitative analysis (adapted from Richards 2013).

Approach	Photointerpretation	Quantitative analysis
Techniques	Visual interpretation	Unsupervised classification, Supervised classification, and Object-based image classification
User	Human analyst	Computer
Scale	Larger than pixel size	At individual pixel size
Area estimates	Inaccurate	Accurate
Spectral resolution	Limited multispectral analysis	Multidimensional analysis
Radiometric resolution	Limited number of distinct brightness levels (4 bit)	All available brightness levels in all features (8, 10, 12 bit)
Shape determination	Easy	Involves complex software decisions

Commonly, photointerpretation involves higher human decision-making level rather than quantitative analysis; however, it brings out lower accuracies (see Table 1). Performing shape determination is easier and faster using photointerpretation, but its reliability depends on the interpreter's skills. Quantitative analysis approach is recommended for bigger data sizes, that include higher spectral and radiometric resolutions. Currently, a set of software with various algorithms is available to process high amounts of imageries data, showing more accurate area estimation than photointerpretation.

1.4. Objectives

The overall objective of this research was to find out the most adequate LC classification method by developing two classification for Jambi province. Two techniques were used: visual interpretation and supervised classification. The study used multi-temporal Landsat-8 satellite imagery sources for both techniques.

Furthermore, the research questions for this study were:

1. What are the main advantages and disadvantages of LC classification for Jambi province, using visual interpretation and supervised classification techniques?
2. What is the best pathway to implement an updated land cover classification using the two different techniques?

2. Study site

Location

The study area is Jambi province. It is located on the eastern coast of Central Sumatra; its capital is Jambi city. Jambi province has an area of 49 144 km^2, that was used for the calculations in this study. Its population is 3 412 265 inhabitants (Badan Pusak Statistik 2010), spread out on its nine regencies and two cities (Jambi and Sungai Penuh).
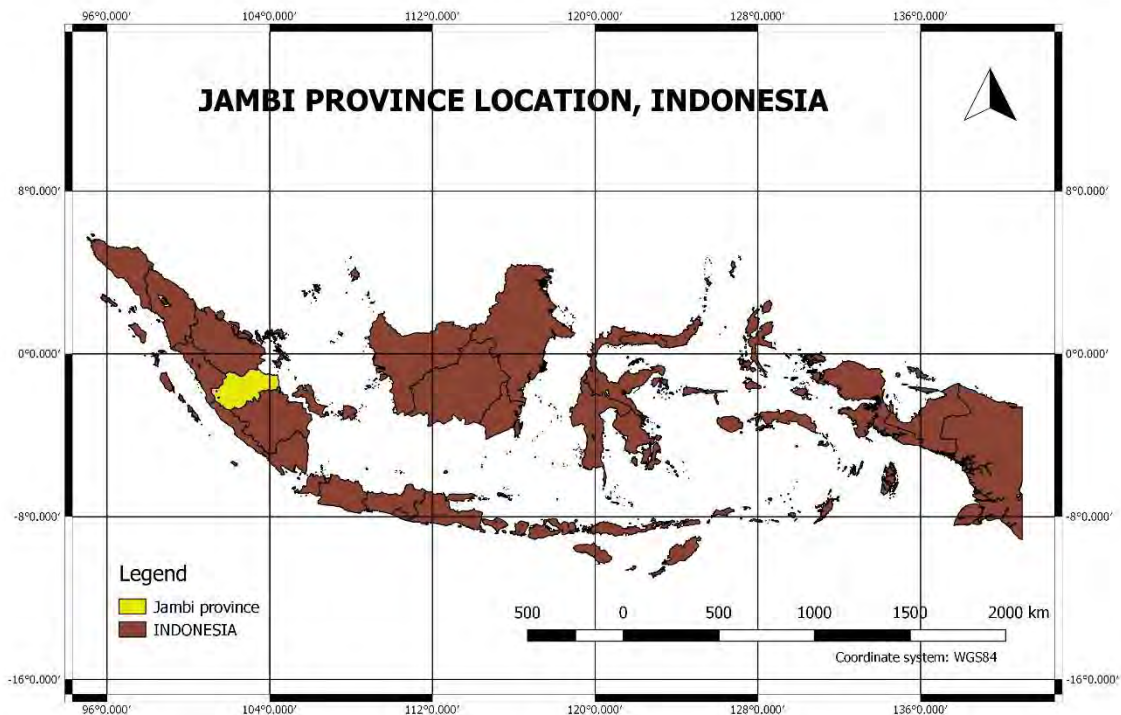
Figure 1 Location of Jambi province. Produced from New Print Composer in QGIS. Coordinate System WGS84.

Climate

According to the Köppen–Geiger climate classification system, Jambi province is a tropical forest (Climate-Data.org 2018), whereas according the Schmidt-Ferguson classification climate type A (Schmidt and Ferguson 1951). The annual precipitation in Jambi city is 2 347 mm with the highest precipitation levels being registered in November, around 270 mm. The driest month is July, with precipitation of between 100 to 110 mm. Precipitation exceeds the evapotranspiration rate for the whole year. The annual average temperature is 26.9 °C, with April being the hottest month with 27.4 °C and January the coldest with 26.2 °C (Climate-Data.org 2018).

4

Geomorphology

The actual geomorphology structure of Sumatra is given by the current subduction of the Indian plate (Barber, Crow, and Milsom 2005). During the quaternary glacial and inter-glacial periods, climatic changes and alteration of the sea level developed Sumatra island (Laumonier 1997). Jambi's altitude goes from the sea level on the eastern coast to the highest point of Mount Sumbing (2 507 meters above sea level – m a.s.l.).

To better understand Jambi province, the island of Sumatra can be divided into the following five natural regions (Verstappen et al. 1973), cited in (Laumonier 1997):

- The coastal strip of the west coast
- The Barisan mountain range and the central graben
- The eastern piedmonts
- The well-drained eastern lowlands
- The eastern swampy lowlands
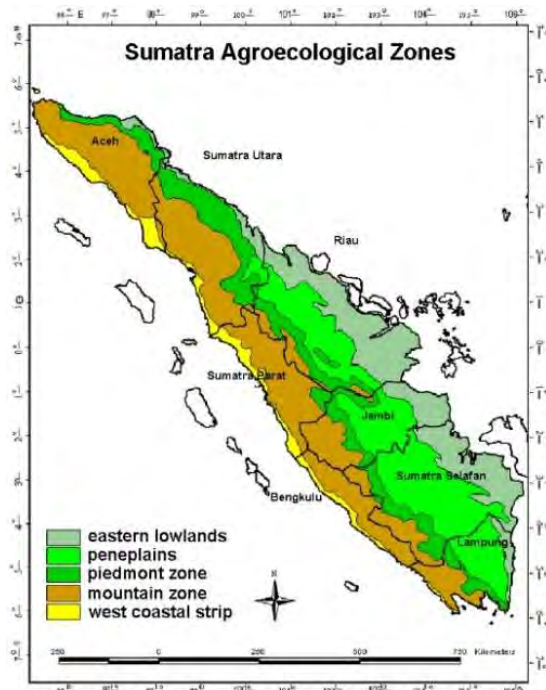
Figure 2 Sumatra Agroecological Zones, five inland zones: eastern lowlands, peneplains, piedmont zone, mountain zone and west coastal strip. Jambi province is located in the central-southern zone of the map (Adapted from Budiwati, Setyawati, and Aries Tanti 2016).

Figure 2 shows five inland natural regions, homologous to the ones explained above: west coast, mountain zone, piedmont, eastern peneplains, and eastern swamp lowlands (Budiwati, Setyawati, and Aries Tanti 2016). For Jambi, the west coast is not included.

Other classifications show comparable features for the province; however, a general division of Jambi is given by two macro-areas: the flat lowland area, dominated by water swamps and peat swamp forests in the east; and the mountain-hilly area, dominated by highland forests in the west (Prasetyo et al. 2016).

Administrative boundaries

Figure 3 shows the 9 regencies of Jambi province as well as Jambi city surrounded by Muaro Jambi regency. Kerinci, parts of Bungo, Merangin, and Sarolangun occupy the mountain zone. Bungo, Tebo, Batang Hari and part of Tanjung Jabung Barat and Muaro Jambi shares the piedmont and peneplains zones. Finally, Tanjung Jabung Timur and part of Muaro Jambi are found in the eastern lowlands (comparing with Figure 2).
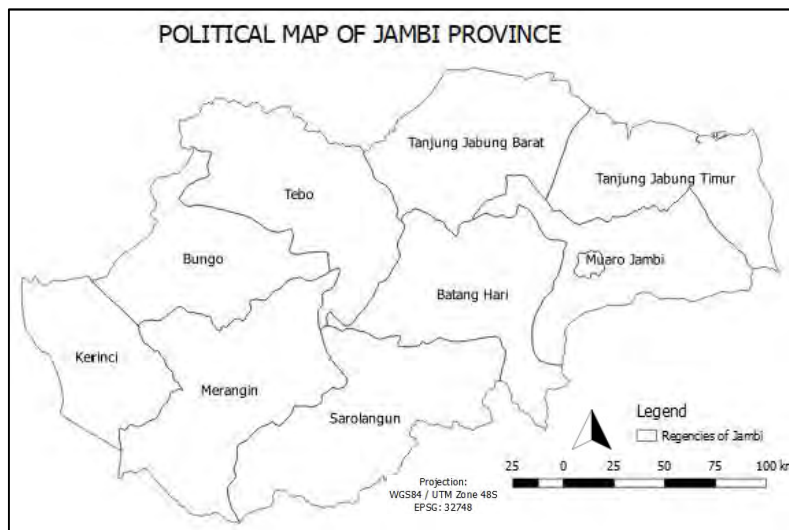
Figure 3 Political map of Jambi province, showing the 9 regencies and one city. Produced from New Print Composer in QGIS. Coordinate System WGS84.

Land cover and land use

As for the national park system, Jambi has two national parks: Berbak that preserves the peat swamp forest in the eastern part of the province, and Bukit Duabelas that preserves the lowland tropical rainforest in the centre part of the province. Other two national parks are shared with other provinces: Bukit Tigapuluh, that protects the lowland tropical forest on the northern part of the province, and Kerinci Seblat, that protects the Barisan mountain range on the western part of the province (Warsi.org 2012).

Indonesia has been experiencing an annual forest loss of 6 800 km^2, from 2010 to 2015, being the second country in the world considering this rate, just after Brazil (9 800 km^2)

and followed by Myanmar (5 500 km^2) (FAO 2016a). In Sumatra island, a deforestation loss rate of 2 900 km^2 has been reached between 2006 to 2012 (Rijal et al. 2016). On the other hand, in Jambi province, between 2006 to 2009, deforestation inside and outside forested areas reached around 770 km^2 per year (Perbatakusuma et al. 2012).

Many drivers of deforestation have been stated in different researches. Between 1980 and 2000, more than 55 % of agricultural expansion in the tropics came from conversion of intact forests, and 28 % of disturbed forests to farm lands (Gibbs et al. 2010). In Sumatra, the national government introduced logging as a systematic business by means of distributing logging concessions (Villamor et al. 2014). Additionally, due to transmigration, Sumatra has lost around 120 000 km^2 of its forests from 1985 to 2007 (Laumonier et al. 2010). Sumatra's land has been transformed for palm oil, rubber, and timber plantations, as well as small-holder agroforestry systems with rubber and fruit trees (van Noordwijk et al. 2017).

The present study states the same LC classes that were identified in the last classification of Jambi province in 2013 by Melati (2018). LC classes are classified for the years 1990, 2000, 2011, and 2013. Areas are presented in percentages in Table 2.

Table 2 Land cover classification for nine classes (visual interpretation) for the years 1990, 2000, 2011, and 2013.

Land cover classes	Extent of Area in squared kilometres (km^2 - %)							
	1990		2000		2011		2013	
Primary forest	13 328.63	27.1	8 852.97	18	8 265.31	16.8	8254.6	16.8
Secondary forest	9 197.25	18.7	8 803.78	17.9	6 579.12	13.4	6 354.49	12.9
Agriculture	7 180.74	14.6	8 705.42	17.7	9 268.89	18.8	9 262.38	18.8
Jungle rubber	983.66	2	245.92	0.5	790.68	1.6	790.68	1.6
Rubber plantation	8 557.87	17.4	8 902.15	18.1	9 660.4	19.6	9 150.33	18.6
Oil palm plantation	3 393.64	6.9	5 557.70	11.3	6 025.95	12.3	5 993.91	12.2
Plantation forest	1 819.78	3.7	1 868.96	3.8	2 078.58	4.2	2 325.94	4.7
Shrub/bush	3 590.37	7.3	4 918.32	10	5 199.2	10.6	5 192.39	10.6
Other	1 082.03	2.2	1 278.76	2.6	1 315.02	2.7	1 858.41	3.8

Table 2 shows a diminution of primary and secondary forest from 1990 to 2013, as well as an increase in agriculture, oil palm plantation, and shrub/bush. The rest of the classes do not present important changes.

Visual interpretation of multi-temporal Landsat imageries was the technique for classification in Table 2.
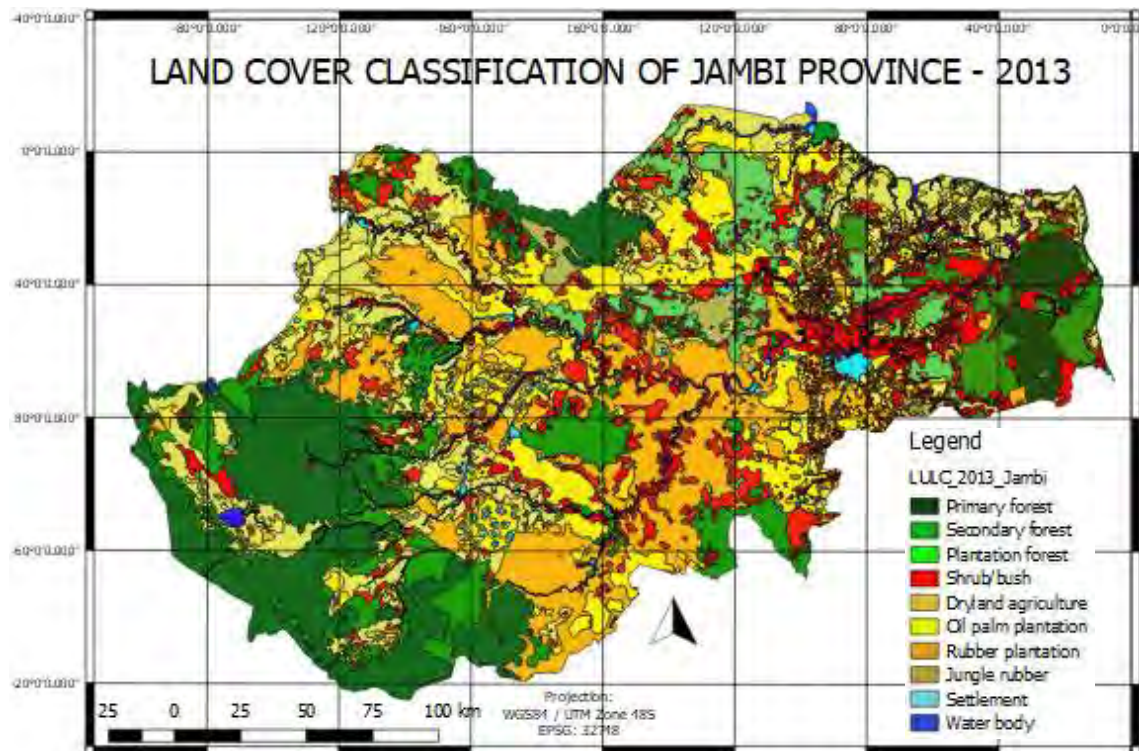
Figure 4 Land use map from 2013 in Jambi province, Sumatra (Melati 2018). Red shades represent natural land classes, yellow shades represent agriculture and agroindustry land classes and green shades represent forests classes. Produced from New Print Composer. Coordinate System WGS84.

Figure 4 shows the forest classes in the western part of Jambi, that coincide with the mountain zone shown in Figure 2. Also, two smaller groups of forested areas are shown in the northern and eastern part of the province. The central part of Jambi province is characterized by rubber and oil palm plantations, mostly agricultural and agroindustry (rubber and oil palm plantations) LC classes. The natural areas defined by shrubs and swamps are spread out all around the province.

3. Materials and methods

For the purpose of this study, two techniques were used: visual interpretation and supervised classification. Therefore, two different classifications are shown and analysed at the end of this research: (1) classification based on photointerpretation approach; and, (2) classification based on quantitative analysis.

Figure 5 shows the pathway of the two techniques used to produce the classifications for the present study.
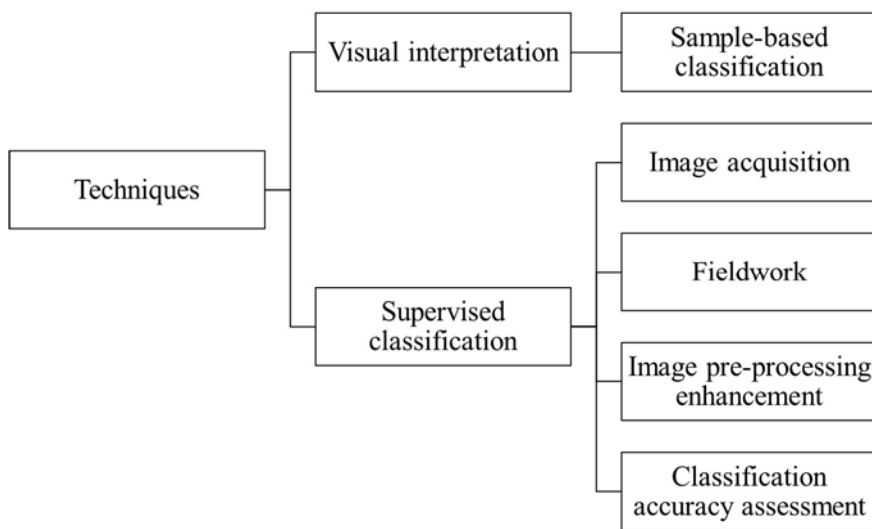
Figure 5 Two techniques for image interpretation: visual interpretation with a single step sample based-classification; and supervised classification with consecutive steps (1) image acquisition, (2) fieldwork, (3) image pre-processing and enhancement, and (4) classification / accuracy assessment.

The first classification was performed under visual interpretation technique. A grid of 1009 plots systematically dispersed was overlaid in the whole province. To analyse the province, a set of multi-temporal satellite imagery from different satellite sources was used (from 2001 to 2017). The overview of the software and tools for analysis is shown in Figure 6. Thus, an LC class was assigned to every single plot. Finally, the results were expressed in: (1) the number of plots per LC class, (2) the percentage that they represent based on the 1 009 plots, (3) the area of each LC class, considering 49 144 km^2 as the total area of the province, and (4) the standard error per LC class.
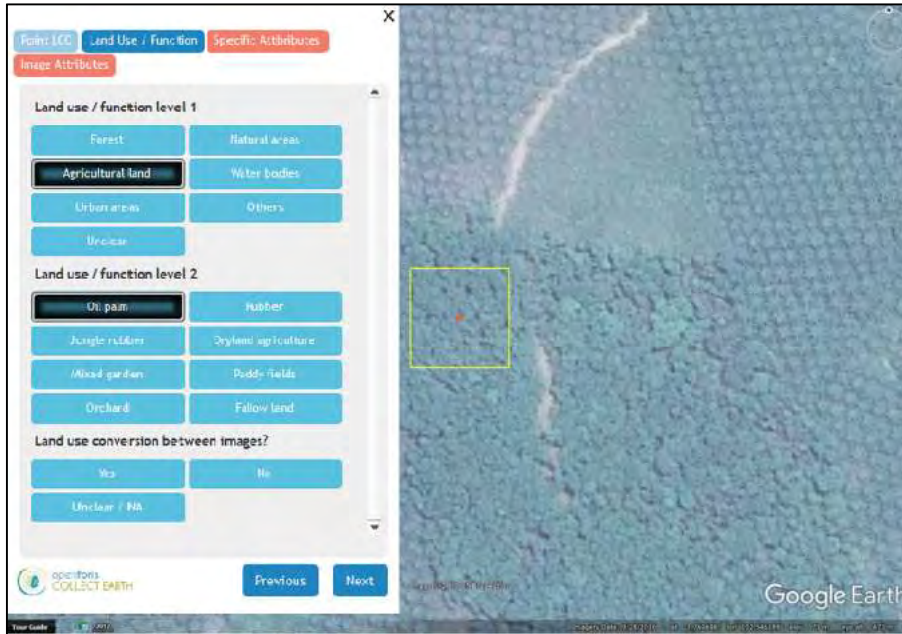
Figure 6 Example of the classification of one plot under visual interpretation technique using Open Foris software tools. Shown options are classified as macro classes in the first set of options and LC classes for the second one. The red dot in the centre and the yellow square (50 x 50 m) are the references for visual interpretation.

The second classification was produced under a supervised classification. A delineated feature using the boundaries of Jambi province (mask) was developed with Landsat-8 satellite imagery from 2018. Reference data was gathered from the field, and spectral signatures per LC class were produced using free remote sensing software. Furthermore, the classification was produced, showing the area that each LC class represents and their percentage in the total classification report. Finally, a confusion matrix was presented to analyse the relative effectiveness of the results.

Needed materials and implemented methodologies are described below.

3.1 Materials

3.1.1 Open and free software
Open Foris – Collect Earth (OF-CE)

OF-CE is a specialized, free, and open source software developed by FAO. It enables data collection through Google Earth. Working together with Google Earth, Bing Maps and

Google Earth Engine, OF-CE allows analysis of high and very high-resolution satellite imagery for many different objectives (FAO 2018), including:

- Support multi-phase National Forest Inventories.
- Land Cover, Land Use Change and Forestry assessments.
- Monitoring agricultural land and urban areas.
- Validation of existing maps.
- Collection of spatially explicit socio-economic data.
- Quantifying deforestation, reforestation, and desertification.

Data collection for LC assessments and monitoring is one of the most important functions of OF-CE. Moreover, it is closely compatible and consistent with IPCC guidelines and UNFCCC mandates (Mendoza et al. 2015).

Because of these characteristics that are not shared with the regular GIS software such as QGIS or ArcGIS, OF-CE was used as the platform to analyse the multi-temporal images for visual interpretation classification,

Google Earth Engine (GEE)

GEE is a cloud-based platform for global-scale earth observation data and analysis (Moore and Hansen 2011). It manages a petabyte-scale dataset, uses JavaScript and Python languages, and contains an online Integrated Development Editor (IDE). GEE has an internal function to generate cloud covers: "ee.Algorithms.Landsat.simplecomposite".

Given that, GEE has its own cloud cover compositing tool and allows extracting a complete polygon that covers Jambi, it was used to download the Landsat-8 satellite image from 2018, instead of the USGS platform (for comparison, see sub-chapter 3.1.2).

QGIS 2.18.12

QGIS (formerly called Quantum GIS) is a free and open-source application for geographic information system (GIS) application. It allows the user viewing, editing, and analysis of geospatial data (QGIS 2016). It also allows analysis and editing of spatial information as tools to generate and export maps. Rasters and vectors can be modified on QGIS, whereas points, lines, and polygons are presented as vectors.

QGIS was used for performing both: Image pre-processing (pan-sharpening) and image enhancement (Principal Component Analysis). Furthermore, the resultant multispectral

image was masked using the Jambi province polygon vector (shown in Figure 9). Additionally, the reference data was transformed into point vectors for the further generation of spectral signatures. Unlike other software, QGIS is a free and open-source, within different tools, and includes the Semi-automatic Classification (SCP).

SCP plugin is also a free open-source for QGIS. It allows performance of supervised and unsupervised classification. It is also useful in running pre and post-classification algorithms, download new images from different satellites (Landsat, Sentinel, MODIS, and ASTER), and raster calculation (Congedo 2016).

For this study, SCP was used to produce the spectral signatures from the reference data brought from the field. Finally, the raster calculation for the supervised classification (produced by Monteverdi 6.6) was run under this tool.

Orfeo Toolbox (OTB) – Monteverdi 6.6

OTB is an open-free source for remote sensing analysis. High spatial and spectral resolution can be processed by OTB. It has a wide set of algorithms that includes pre-processing imagery, such as ortho-rectification, any kind of image enhancement, or classifications. All the algorithms from OTB can be visualized on Monteverdi app.

Given that QGIS cannot process big sized imagery for classification algorithms (the final satellite mosaic image had around 6 to 7 GB size), Monteverdi 6.6 app was used to process the classification and accuracy assessment after the spectral signatures were ready.

3.1.2 Set of multi-temporal imagery

For visual interpretation technique, a set of multi-temporal satellite imagery was used to elaborate the classification. The satellite sources were: Airbus, CNES, Copernicus, Digital Globe, Landsat program, MODIS, Rapid Eye and Sentinel. For each plot, several satellite sources were used to identify the LC class, however, only one of them was chosen to confirm the definitive LC class allocation. 53 % of the plots were identified using Landsat imagery, 27.5 % by Digital Globe, 18.5 % by CNES/Copernicus, and 1 % by other satellite sources.

Besides the LC classification by visual interpretation technique, the Moderate Resolution Imaging Spectroradiometer (MODIS) sensor was used to identify and quantify fire warnings. MODIS is a sensor from the Earth Observing System (EOS) of the National

Aeronautics and Space Administration (NASA), that is used for researches whose topics are fire detection, land cover change, and land surface temperature, among other topics (Justice et al. 2002).

For supervised classification technique, only Landsat-8 satellite imagery from 2018 was used to create a digital mosaic, that covers the whole province. This sensor has a spectral resolution of eleven bands, including VIS, NIR, SWIR, TIRS, and one panchromatic band. It has variable spatial resolutions: 30 m (VIS, NIR, and SWIR), 100 m (TIRS) and 15 m (panchromatic). The radiometric resolution is 12 bits and the temporal resolution is 16 days (USGS 2018b).

Table 3 Bands used in this study (from 2 to 8). Wavelengths are shown in micrometres (µm) and spatial resolution in meters (m).

Bands	Wavelength (µm)	Resolution (m)
Band 2 – Blue	0.452 - 0.512	30
Band 3 – Green	0.533 - 0.590	30
Band 4 – Red	0.636 - 0.673	30
Band 5 - Near Infrared (NIR)	0.851 - 0.879	30
Band 6 - Shortwave Infrared (SWIR) 1	1.566 - 1.651	30
Band 7 - Shortwave Infrared (SWIR) 2	2.107 - 2.294	30
Band 8 – Panchromatic	0.503 - 0.676	15

The bands used in this study are listed in Table 3. It was important to consider all the bands to perform the final image for the classification. Bands 2, 3, and 4 were used to have an overview of natural colour while performing the classification on the image. Band 5 was considered to eventually perform vegetation indices such as NDVI. Bands 6 and 7 were included because of their wavelengths, that avoid cirrus clouds. Band 8 or panchromatic (PAN) band was used for a further image pre/processing. A PAN band is a single spectral band, that normally expands up to the wavelengths of two or more visible or infra-red bands (Khan Rahaman, Quazi Hassan, and M. Ahmed 2017). This characteristic gives the opportunity to pan-sharpen the rest of the bands with lower spatial resolution.

Five Landsat-8 imageries are required to mask the satellite image mosaic into the whole Jambi province (see Figure 7). The imagery is available from the United States Geological Survey (USGS 2018a), which classifies Landsat imagery locations by paths (P) and rows

(R). Figure 7 shows the position of P and R for Jambi province, called location for this study.
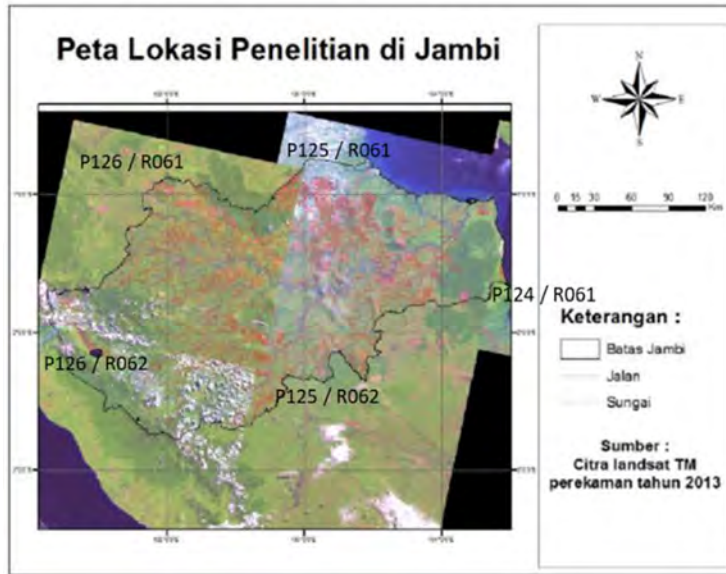
Figure 7 Set of five locations to cover the whole of Jambi province: P124/R061, P125/R061, P125/R062, P126/R061 and, P126/R062 (Wijaya, Saleh, and Tiryana 2015).

Indonesia does not have a seasonally cloud-free window, therefore more data is required to overlay the cloud patches on the imagery mosaic (Margono et al. 2012). Consequently, generating a satellite image mosaic with features from the same day, week or month was not possible. Cloud covers above 50 % of the imagery were found during this study. When images from different dates were overlaid, different patterns of colour were distinguished within the province. Figure 8 shows the differences in colour patterns, limited from the different locations indicated in Figure 7. Location P125/R061 shows a marked red shape, whereas P126/R061 is characterized by a bright shade, and P126/R02 has the darkest shade.

Even when the resultant image had less cloud coverage after the mosaicking process (merging imageries from different positions and delineating them using the Jambi province vector as reference), it was impossible to equalize the colour patterns to reduce these differences. An additional characteristic of this satellite image mosaic was that almost all the imagery was gathered from 2016 (only one image was from 2017).
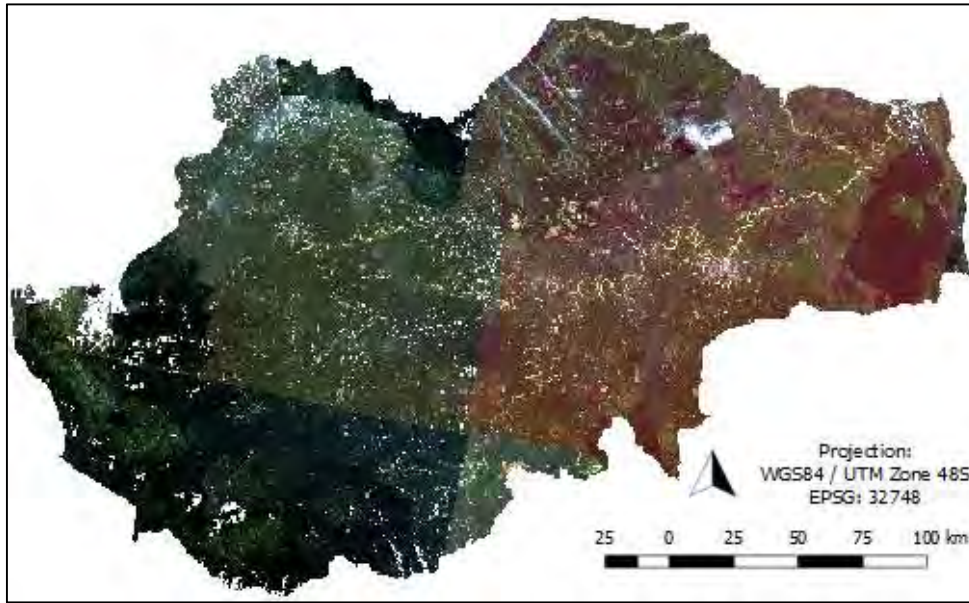
Figure 8 Jambi mask from seven different Landsat-8 satellite imagery (natural colour). Seven images were overlaid to produce the final mosaic. Produced from New Print Composer in QGIS. Coordinate System WGS84.

One Landsat-8 imagery square was used to assemble the image mosaic to cover the entire Jambi province surface. The initial mosaic was obtained from GEE based on images from 2018 (from January to September), the cloud cover was already masked by the software. It also considered the five locations indicated in Figure 7.
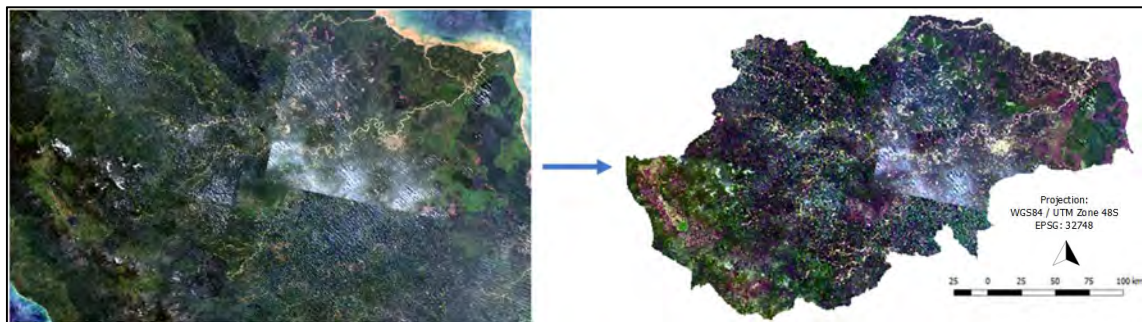
Figure 9 Lansat-8 satellite image mosaic from 2018 and the further masking for Jambi province mosaic (natural colour). Produced from New Print Composer in QGIS. Coordinate System WGS84.

Figure 9 shows the final image mosaic mask developed for the supervised classification. Even though the cloud cover is higher than the mask from Figure 8, this is the most recent image (2018), it includes a basic cloud composite called "simple composite Landsat Google Earth Engine", and the same colour patterns within the image. "Clipper" tool from QGIS was run to mask the image into Jambi province vector. Finally, the resultant mosaic was saved as a .tiff format. However, a clear bright pattern is visible in part of the eastern side of Jambi, where the location P125/R061 is settled.

3.2 Methods

Since the results of this study are two land cover classifications under two different techniques, the methods are presented as follows:

The sub-chapter 3.2.1 explains the methods for the first technique; whereas the second technique is explained under the stated remote sensing workflow by Magdon et al. (2017):

- Image acquisition: explained already within the sub-chapter 3.1.2.
- Image pre-processing and enhancement: explained in sub-chapter 3.2.2.
- Assessment of reference data: explained in sub-chapter 3.2.3.
- Classification and accuracy assessment: explained in sub-chapter 3.2.4.

3.2.1 Sample based analysis

For this phase, visual interpretation was considered. This technique selects key elements such as trees, palm trees, bushes, rivers, among others, as ancillary components to allocate a class to a delimited area. Thus, using GIS software, an area is compared with the key element and consequently classified. (Margono et al. 2016). OF-CE was used for the classification. For this study, a squared grid layer of 1 009 plots, distanced 7 km from each other, was overlaid in the whole province. For the assessment, a set of multitemporal satellite imagery sources, stated in subchapter 3.1.2, were analysed.

This classification was performed on August 2017, by analysing the most recent and available satellite imagery possible. In the case where a recent image was not clear enough for class identification, the nearest older image was selected instead. The main idea was to keep the sources as recent as possible. For this classification, two kinds of coverage were identified (see Figure 6): (1) What was in the red dot of the plot, and, (2) What was in the green square. The surrounding area was managed as a reference for the user. For effects of the results, the coverage within the green square (50 x 50 m) was included in the report. Results from the red dot are indicated in annex 02.

The classification key for this part is illustrated in Figure 10. Six macro-classes and the option for unclear plots are shown. Unclear point means that either due to cloud cover or image resolution, it was not possible to assign an LC for the corresponding plot. The forest macro-class contained five different classes including primary and secondary

forests; natural areas included combinations of shrubs, swamps, and grasslands; agricultural land was subdivided into regular agriculture and agroindustry crops such as rubber or oil palm plantations; water bodies and urban areas did not have sub-divisions, whereas others included mining, open/bare lands, and Trees Outside the Forest (TOF).

Additionally, each plot was analysed using the MODIS sensor. By identifying the NDVI value and other tests, it was possible to identify "fire pixels" (Giglio et al. 2003). Several improvements have been done for the MODIS sensor for fire detection, hence, it is recommended to use data acquired from November 2000 (Giglio, Schroeder, and Justice 2016). For this study, every plot was analysed in order to count the number of fire warnings per year and register them into the database.
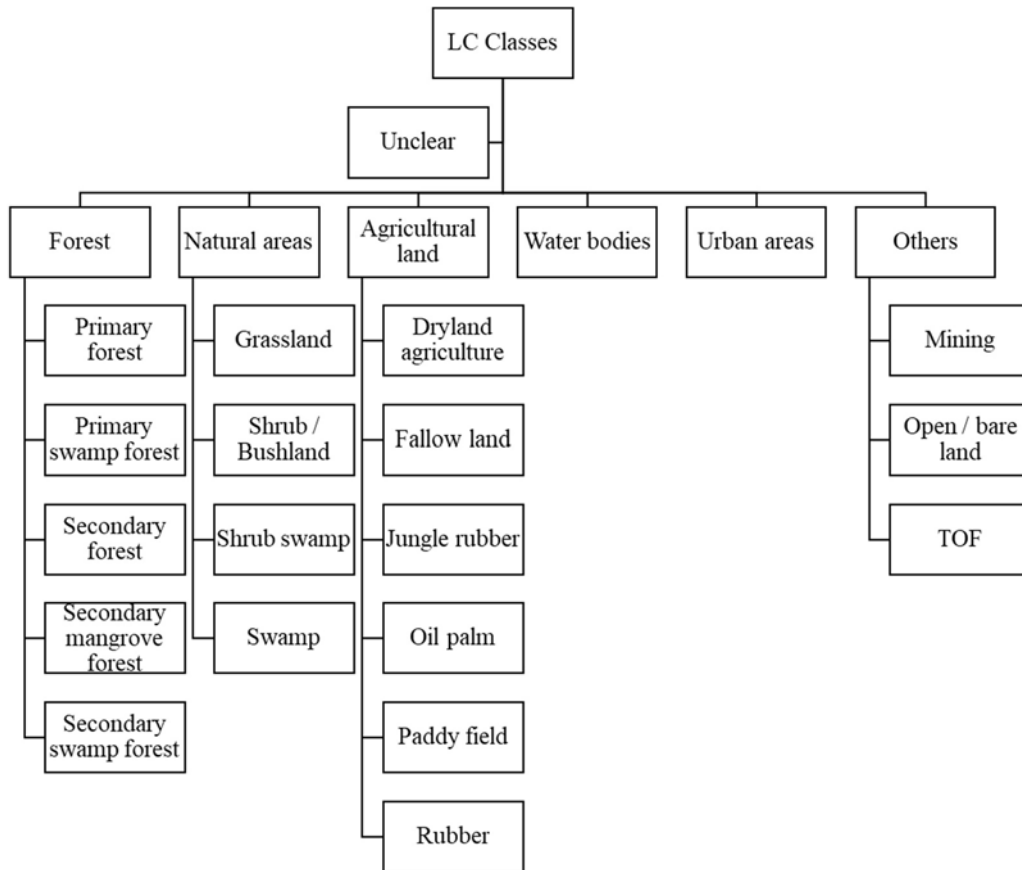
Figure 10 Classification key for sample-based classification, with 6 macro-classes, 18 LC classes, and an extra class for unclear images.

3.2.2 Image pre-processing and enhancement

Pan-sharpening

The spatial resolution is defined as the pixel size of an image (Richards 2013). As shown in Table 3, the spatial resolution of Landsat-8 images for bands from 2 to 7 is 30 meters and 15 m for band 8 (PAN band).

Pan-sharpening is a fusion technique to enhance images, by combining a PAN image of high spatial resolution with multispectral image data of lower spatial resolution (Ehlers et al. 2010). Interpretability and utility of the multispectral data is the result of pan-sharpening enhancement (Laben and Brower 2000).

Using pan-sharpening (Bayes) algorithm (from QGIS), the multilayer Landsat-8 satellite image mosaic was pan-sharpened to increase spatial resolution from 30 m to 15 m. Pan-sharpening is mostly used for visual purposes (Johnson 2014). For this study, besides the supervised classification, pan-sharpened mosaic image in natural colour was used to compare 2013 classification, visual interpretation, and supervised classification results.

Principal components analysis (PCA)

Bands of multispectral images are often correlated, and it brings redundant information between them. Conventional satellites like Landsat could supply data with a few percentages of overlapping information between adjacent bands (Wang, Tyo, and Hayat 2007). The greatest advantage of PCA is that it detects patterns between the bands, and therefore accentuates their similarities and differences into a final product (Gupta et al. 2013). The PCA follows these concepts and converts the original data to reduce the correlation between bands (Rodarmel and Shan 2002). For instance, imagery information, such as the presence of vegetation and forestry area with fire damages, is feasible to detect using PCA (Estornell, Sebastiá, and Mengual 2013). Also, PCA can even distinguish an isolated riparian forest surrounded by a hilly prairie mountain (Henebry 2014).

However, PCA has some disadvantages, such as scene dependence, this means: when different imageries of the same region are acquired at different times or seasons, the resultant PCA image could vary depending on the behaviour of the pixel, even if the area remains unchanged (Gupta et al. 2013).

PCA was run with the multi-spectral satellite mosaic image (forming the 7 bands), using four components on the OTB tool "Dimensionality Reduction (PCA)", under QGIS software. This enhancement process was applied for the complete satellite imagery mosaic, consequently, no problems linked to times or seasons were reported. The output raster was used for further classification.

3.2.3 Assessment of reference data

Selection of reference source

The planning of this phase started in March 2018. To generate a base map that gathers all the interesting classes to visit, the 2013 LC map (Figure 4) was used to identify the former LC class distribution. The closest LC classes to the Jambi city (red polygon in Figure 11) were selected as reference sources. Furthermore, ten concentrically circular buffers of ascending radios from 10 to 100 km radius were overlaid on the base map. The second buffer was done by overlaying the main roads around Jambi city in the base map. The classes that intersected with the main roads were selected as sample classes. The main considerations for this selection were: (1) the easy accessibility of the LC areas, with regards to the selected main roads, and (2) the inclusion of all the classes in the sampling. The road system was divided into four cardinal directions: south, west, north-west, and east.

To confirm whether the LC classes were still the same or not, two sources were used:

- The results of the visual interpretation classification (explained in sub-chapter 3.2.1 and exposed in sub-chapter 4.1).
- Review of the Landsat satellite image mosaic from 2018 (see Figure 9).

This distribution of the sample classes among the four main roads (Figure 11) was used to ensure that all the LC classes were visited, hence, gathering many points per class.

Figure 11 shows the base map: NDVI map as background, the four road matrices of Jambi province in white shape, and the ten concentrically circular buffers distanced 10 km from each other.
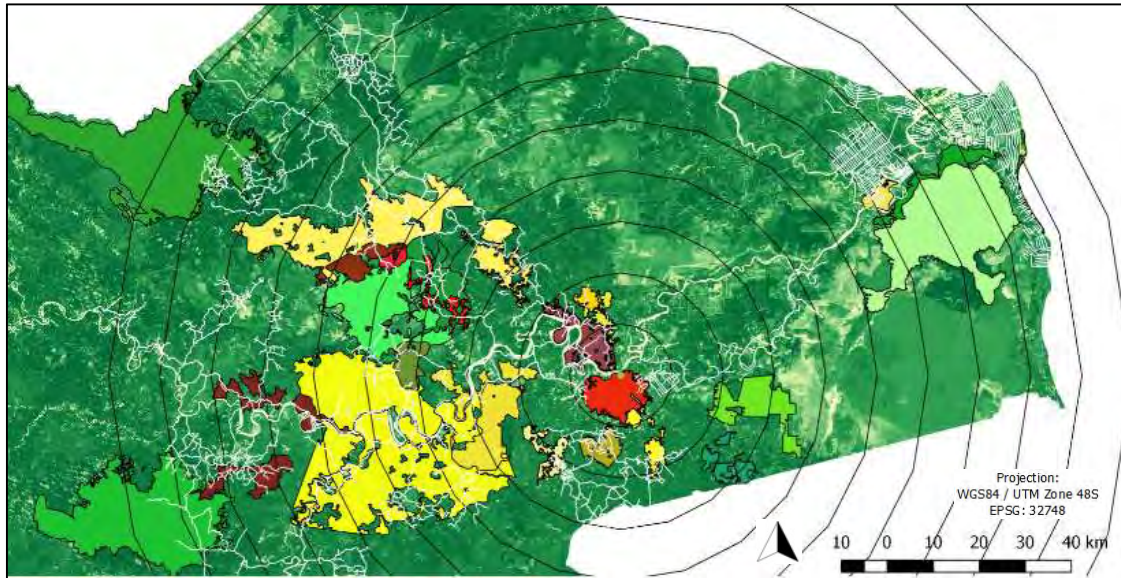
Figure 11 Sampled areas including all the land cover classes, based on land cover classes from 2013 classification with two buffers: concentrically circles and road matrix (in white). Forest classes in green shades, agricultural classes in yellow shades and natural areas classes in rod shades. Produced from New Print Composer in QGIS. Coordinate System WGS84.

According to the four road matrices, the first one indicates the southern road with 7 different classes, the second one is the western road with 7 different classes, the third one is the north-western road with 11 different classes, and the fourth one is the eastern road with 7 different classes. In total, this map contains 22 different classes.

The LC classes to be gathered from the field were grouped into macro-classes. A total of 6 macro-classes and 25 LC classes were identified (see Figure 12). The six macro-classes were the same than those evaluated with visual interpretation technique (see Figure 10). However, for the purpose of this study and concerning the classification from 2013, several of these LC classes were either merged or excluded to get ten final LC classes. The matrix that includes all the points gathered in the field (with the classification key from Figure 12) is indicated in Annex 03.

Furthermore, some characteristics for the gathered data were the following:

- The same number of reference points per class.
- A minimum distance of 200 m between reference points (to avoid pseudo-replication and to increase generality of the reference data).
- Select the centre of larger patches that are likely not mixed classes.

20

- A minimum of between 30 to 50 points per class.[1] For multispectral images, pixel number sample (n) must vary between 10 to 100 (Richards 2013).
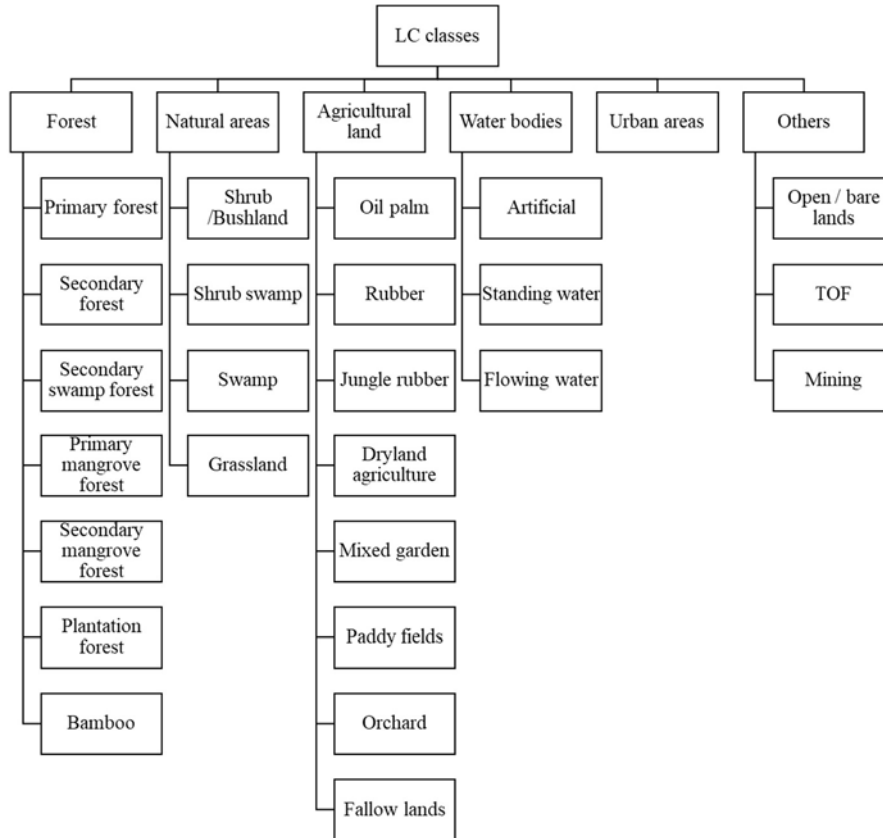
Figure 12 Classification key for supervised classification technique, showing 6 macro-classes and 25 LC classes.

Fieldwork

In this section, the main tasks for the fieldwork are summarized according to the Guidelines and Field Protocol generated by CRC990 subproject B05[2].

The most important devices are listed below:

- Samsung Tab Active2 (8.0, LTE) (SM-T395N). Samsung. South Korea.
- Trimble Juno 3B, GeoMobile, United States of America.
- TruPulse® 360º Rangefinder, Laser Technology Inc. United States of America.

---

[1] Smaller numbers in rare classes and higher numbers in frequent classes give more accuracy and weight to frequent classes at the cost of rare classes but may enhance the overall accuracy of the map.
[2] Unpublished document

- Garmin GPSMap 64st, Garmin Ltd., United States of America.
- Dendrometer II, Department of Forest Inventory and Remote Sensing of University of Göttingen, Germany.

Fieldwork was carried out in July 2018, the driest month according to chapter 2. This phase consisted of the data collection through a digital survey uploaded on a Samsung Tab Active2. Thus, points for reference data were taken for different LC classes. The operation of the devices consisted of linking the TruPulse® 360º Rangefinder (laser device) with the Trimble Juno 3B. Therefore, when aiming at an area with the laser device, the coordinates were automatically recorded on the Trimble Juno 3B. Once the coordinates for a point were gathered, the LC class was identified and filled in the Samsung Tab Active2's survey. The distance between the observer and the point could reach up to 500 m.

Besides the LC identification, several characteristics about the visiting area and its surroundings were gathered. Additionally, for the case of forest classes, extra features were included such as vertical structure, management and/or damages, among others. Also, the basal area was measured for forest LC classes and rubber plantations using the Dendrometer II.

Garmin GPSMap 64st receiver was used for the navigation and allocation of each sample point when Trimble Juno 3B was not needed (not remote distances required).

These gathered points (reference data) were randomly divided into two groups with the same number of points. These two groups were used to perform the classification (training points) and the accuracy assessment (validation points). Finally, ten different classes were selected for the supervised classification process: primary forest, secondary forest, plantation forest, natural areas, agriculture, oil palm, rubber, jungle rubber, urban areas, and water bodies. The first eight classes were the same as in the 2013 classification, its ninth class was "others", that includes urban areas and water bodies.

3.2.4. Classification and accuracy assessment
Supervised classification

Supervised classification is the most commonly used technique for quantitative evaluation of satellite image data. It is based on the assumption that each class can be

identified as a probability, by a distribution in a multispectral space (Richards 2013). Spectral of the domain can be defined as the collection of spectra, where every pixel represents a vector, whose components are reflectance values from a particular wavelength (Fauvel 2008). Supervised classification also requires previous or a priori knowledge (reference data) about the region, where real field information is taken (Kim 2016). For this study, the second classification was obtained using supervised classification. A further map is additionally presented in chapter 5.

For better understanding, Figure 13 shows the workflow of the supervised classification process, that also includes accuracy assessment. According to the Figure 13 (Lillesand, Kiefer, and Chipman 2007), the classification is implemented in a multispectral image of 5 bands or channels, which means that each pixel has 5 different digital numbers (DN_1, DN_2, D_3, DN_4, and DN_5). During the training stage (1), the user indicates the classes to classify and collects field data from every different land class. Water (W), sand (S), forest (F), urban (U), corn (C), and hay (H) are stated. The selection of the LC classes and the operation of the reference data gathering have been detailed in sub-chapter 3.2.3.
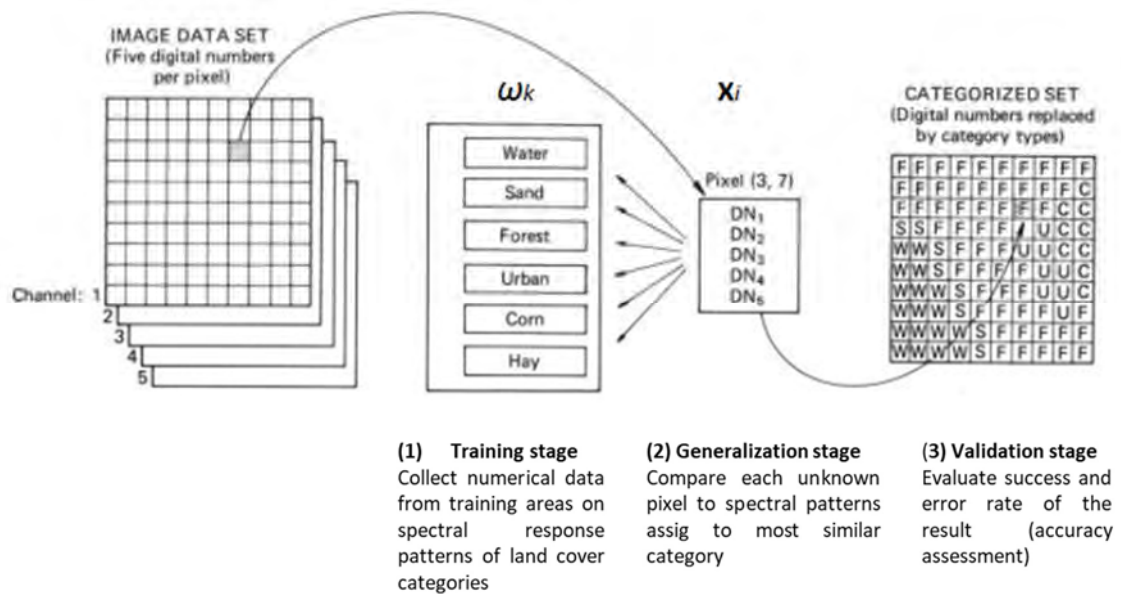
Figure 13 Supervised classification workflow, showing: a multispectral image of five channels or bands, training stage for 6 classes (water, sand, forest, urban, corn, and hay), generalization stage with five DNs of one pixel, and validation stage with all the classified pixels: 18 water, 8 sand, 56 forest, 8 urban, 9 corn, and 1 unclear pixel (Source: Lillesand, Kiefer, and Chipman 2007).

During the generalization stage (2), each pixel is assigned to the most similar land class according to the training data by comparing their DN. This stage is made using the

classifier or classification algorithm. Finally, during the validation stage (3) / accuracy assessment, the quality of the map and the classification itself is assessed.

For this study, the Semi-Automatic Classification Plugin (SCP) from QGIS was used to generate the spectral signatures per class. SCP allows the user to (1) define classification inputs, (2) collect regions of interest (ROIs) and spectral signatures, and (3) assess spectral signatures. These three steps were the preparation for the classification process itself. Spectral signatures were assessed for training and accuracy points.

SCP uses the automatic region growing algorithm. According to this algorithm, the user selects a point manually in each target area (LC class). In order to increase the area, the surrounded pixels should be highly similar to the point, then the rest of the pixels can be classified as the same LC as the training data (Q. Li, Wei, and Zhao 2017).

The present classification was executed using Random Forest (RF) classifier. This classifier produces several decision trees, extracting randomly a set of training points and variables or classes (Belgiu and Drăguţ 2016). Each tree selects the most popular class for the pixel that is to be classified (Pal 2005).

Meanwhile, Monteverdi 6.6 was the software selected for the classification process using the RF classifier. Image statistics and the model for classification were prepared by the OTB tools of this software before the final classification.

Accuracy assessment

Accuracy assessment states the comparison between the land map classification and a higher quality reference data. (FAO 2016b). It helps in understanding, for instance, how reliable a classified vegetation class could be (Summer and Nordman 2008). Therefore, the map with higher indices of reliability will be the better for practical uses.

Since the reference data from the field was divided into two different groups with the same number of points, both datasets were independent of each other.

A regular way to present the accuracy assessment is by undertaking it tabularly in a confusion matrix. The values on the matrix represent the number of truth pixels from the ground per class, correctly and incorrectly assigned by the classifier (Richards 2013). Table 4 shows the scheme for presenting the confusion matrix for this study.

Table 4 Confusion matrix example, showing the accuracy assessment for 5 LC classes.

	ID_Class	1	2	3	4	5	Ref_Tot	PA (%)
					Classified			
Reference	1	**34**			3	2	39	87.2
	2		**12**				12	100.0
	3			**13**	8	1	22	59.1
	4		1	3	**46**		50	92.0
	5	1			2	**25**	28	89.3
	Class_Tot	35	13	16	59	28	151	
	UA (%)	97.1	92.3	81.3	78.0	89.3	OA	86.1

According to Table 4, a classification of five classes has been produced. The highlighted numbers are the pixels that have been correctly classified, whereas the other ones are incorrectly classified for the classes that cross them. The User Accuracy (UA) represents the reliability of different classes in the map for the map user. For instance, 13 from 16 pixels in the map (class 3), have been correctly classified; $UA_3(13/16)$ x 100 = 81.3 %. The Producer Accuracy (PA) represents the performance of the mapping process to the analyst. For example, for the same class, 13 from 22 pixels from the reference have been correctly classified; $PA_3(13/22)$ x 100 = 59.1 %. Finally, the Overall Assessment (OA) indicates the relative effectiveness of the classification.

4. Results

4.1 Sample based analysis

After the visual interpretation classification, 1009 plots were classified based on the classification key stated in Figure 10. The results are shown in Table 5. Macro-classes, LC classes, number of classified plots (n), the proportion (p) between n and 1 009 plots, area, and standard error (SE) are indicated per LC class.

Table 5 Visual interpretation results showing the number of classified plots (n), proportions (p) based on the total area of Jambi province, the area, and standard error (SE) per seven macro-classes and twenty-six classes.

Macro-class	LC class	n	p (%)	Area (km^2)	SE (%)
Forest	Primary forest	164	16.25	7 988	7.15
	Primary swamp forest	1	0.10	49	99.95
	Secondary forest	300	29.73	14 612	4.84
	Secondary mangrove forest	1	0.10	49	99.95
	Secondary swamp forest	5	0.50	244	44.61
	Unclassified	3	0.30	146	57.65
Natural areas	Grassland	13	1.29	633	27.56
	Shrub/bushland	87	8.62	4 237	10.25
	Shrub swamp	11	1.09	536	29.99
	Swamp	2	0.20	97	70.64
	Unclassified	1	0.10	49	99.95
Agricultural land	Dryland agriculture	55	5.45	2 679	13.11
	Fallow land	14	1.39	682	26.54
	Jungle rubber	2	0.20	97	70.64
	Oil palm	125	12.39	6 088	8.37
	Paddy fields	5	0.50	244	44.61
	Rubber	25	2.48	1 218	19.75
	Unclassified	28	2.78	1 364	18.63
Water bodies	Water bodies	13	1.29	633	27.56
Urban areas	Urban areas	13	1.29	633	27.56
Others	Mining	2	0.20	97	70.64
	Open/bare land	44	4.36	2 143	14.74
	TOF	9	0.89	438	33.18
	Unclassified	1	0.10	49	99.95
Unclear	Clouds	6	0.59	292	40.7
	Image resolution	79	7.83	3 848	10.8
		1009	100.00	49 144	

Per LC class

According to Table 5, primary forest, secondary forest, oil palm, and shrub/bushland were the most frequently classified LC classes. These four classes represented 67 % of the total area of the province. Dryland agriculture and rubber are worth mentioning because of the high number of plots they occurred (55 and 25 respectively). Given that their numbers of plots do not represent as much area as the rest, water bodies and urban areas are macro-classes without subdivision. Together, they covered only 2.58 % of the whole province.

Four out of six macro-classes contained the LC class "unclassified". Even though, "forest", "natural areas", and "others" macro-classes did not contain more than three plots with this sub-classification, "agricultural land" included 28 plots, that represents 2.78 % of the total classification and 11.02 % of the macro-class.

In order to identify the plots with difficulty in assigning classes, the "unclear" division was added to Table 5. Cloud cover and image resolution were the factors that influenced this misidentification. It was impossible to assign a macro-class for a total of 85 plots, a fact that represents the 8.42 % of the plots (0.59 % for clouds and 7.83 % for image resolution).

To estimate the different areas per LC class, the total area of Jambi province was multiplied by the factor of the "n" divided under the 1 009 plots (expressed as p in Table 5). Each area estimation is indicated in Table 5.

The standard error (SE) is the percentage estimated between the standard deviation and the squared root of the number of plots per LC class. The higher the n, the lower the SE. Since the SE indicates the reliability of the mean, a low SE value showed better accuracy in regards of the total population. Therefore, the secondary forest had the lowest SE (4.84 %) followed by primary forest (7.15 %), oil palm (8.37 %), and shrub/bushland (10.25 %). Another way round, less represented LC classes such as paddy fields or secondary swamp forest were classified in 5 plots each, and their SE was 44.61 %. The extreme case is shown when the LC had only one plot (secondary mangrove forest), and the SE was 99.98 %.

By comparing the results from Table 5 with Melati's classification (Table 2), an important increment for oil palm, from 1990 to 2000 (6.90 to 11.30 %) and a small percentage decrement from 2011 to 2013 were observed, with coverages of 12.30 and 12.20 %

respectively. Meanwhile, a value of 12.4 % was reported in the visual interpretation classification. For primary forest, equal values of 16.8 % in 2011 and 2013 were presented, whereas 16.25 % was shown in this classification. In the case of jungle rubber LC class, Table 2 showed 1.60 % in 2011 and 2013, whereas 0.20 % of the total province was covered in this classification.

Following the comparison, the secondary forest covered 30.33 % of Jambi, whereas Table 2 stated that, the values of this LC class decreased from 17.90 % (2000) to 13.40 % (2011), and finally with a further low decrease into 12.90 % (2013).

For agriculture analysis, the macro-class "agricultural land" (Table 5) contained several LC classes that could be grouped. Hence, summarizing "dryland agriculture", "fallow land", and "paddy fields", the final value was 7.34 %. Meanwhile, Table 2 showed that "agriculture" changed from 14.6 % (1990) to 18.8 % (2013), both higher than the one from this classification. Finally, rubber plantation LC class has had a stable evolution through 1990 to 2013 (between 17 to 19 % approximately), but only 2.48 % in the visual interpretation results, much less than the past years.

Per Macro-class

To summarize the results and to interpret them at the macro-class level, Table 6 shows the distribution of classified plots per macro-class (n), the area that they occupy, the proportion in the percentage that they represent in the whole province (p), and the SE.

Table 6 Visual interpretation results summarized from macro-classes (based on results from Table 5).

Macro-class	n	Area (km^2)	p (%)	SE (%)
Forest	474	23 086	49.98	3.34
Natural areas	114	5 552	11.30	8.86
Agricultural land	254	12 371	25.17	5.43
Water bodies	13	633	1.29	27.56
Urban areas	13	633	1.29	27.56
Others	56	2 728	5.55	13.11
Unclear	85	4 140	8.42	10.31
TOTAL	1 009	49 144	100.00	

Forest occupied almost half of the whole province (49.98 %), while agricultural land was represented as the fourth part of Jambi (25.17 %). Their SE values are also the lowest ones. Natural areas represented 11.30 % of the classification, others macro-class was 5.55

%, whereas water bodies and urban areas each summed up to 1.29 %. The six main macro-classes represented 91.58 % of all the classification, while the rest of the area was presented by unclear (8.42 %) macro class. Likewise, in Table 5, the higher the n value, the lower the SE.

In the 2013 LC classification (Table 2), the forest classes (primary forest, secondary forest, and plantation forest) added up to 34.4 %, for natural areas (shrub/bushland) was 10.6 %, agricultural land (agriculture, jungle rubber, rubber plantation, and oil palm) was 51.2 %, and others was 3.8 %. Hence marked differences were found in this visual interpretation classification. Consequently, for visual interpretation classification, forest macro class was higher whereas agricultural land was lower than 2013 classification. Natural areas remained relatively constant while others slightly varied.

Per regency

Regarding the distribution of macro-classes per regency, as it is shown in Table 7, the highest percentages of forests were in the three regencies on the west of Jambi: Kerinci, Merangin, and Sarolangun with 63 %, 67 %, and 61 % of forest cover respectively.

Table 7 Visual interpretation results, distributing macro-classes per regency and Jambi city (in percentage).

Regencies	Forest (%)	Natural areas (%)	Agricultural land (%)	Water bodies (%)	Urban areas (%)	Others (%)	Unclear (%)
Batang hari	51	8	20	4		8	9
Bungo	49	20	19	1	3	3	5
Jambi	25		50		25		
Kerinci	63	18	8	3	1		8
Merangin	67	15	12	1		3	2
Muaro Jambi	40	4	32		3	13	8
Sarolangun	61	10	18	1	1	6	3
Tanjung Jabung Barat	25	5	50	2	1	4	15
Tanjung Jabung Timur	23	6	53	1		7	10
Tebo	39	17	19	1	2	5	18

The regencies with the highest incidence of agricultural land plots were the ones located in the north-eastern side of Jambi (see Figure 3): Tanjung Jabung Barat (50 %) and Tanjung Jabung Timur (53 %) regencies. Jambi city also had a high percentage of this

macro-class, however, it had only four plots, hence, its reliability is not adequate for this analysis.

Natural areas were mostly registered in Bungo, Kerinci, and Tebo (north-west). Both regencies, Tebo and Tanjung Jabung Barat in the north of the province, presented the most unclear images for this classification. Figure 14 shows the distribution of the macro-classes in the different regencies of Jambi province.
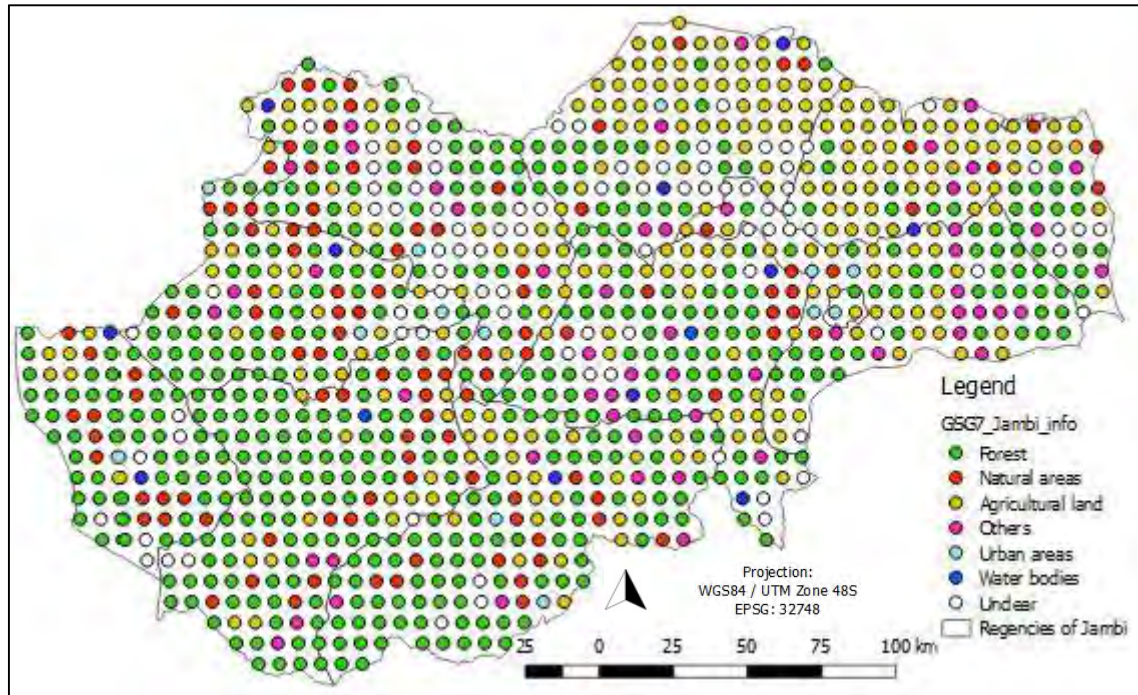

Figure 14 Visual interpretation results, distribution of classified macro-classes in Jambi province. Regency boundaries are shown. Green dots represent forest macro-class, red dots for natural areas, yellow dots for agricultural land, pink dots for others, light blue dots for urban areas, blue dots for water bodies and white dos for unclear plots

Figure 14 showed green shaded plots (forests) mostly distributed on the western side of Jambi, agricultural land highly distributed on the north-eastern side, and the rest were unevenly distributed across the province.

When overlapping Figure 14 on 2013 classification (Figure 4), 71 secondary forest plots and 14 unclear plots were located where rubber plantation was classified in 2013. Furthermore, 20 palm oil, 6 secondary forest, 5 unclear, 4 fallow lands, 3 rubber plantation, and a remaining 6 more plots were distributed where plantation forest class was allocated in 2013. Plantation forest LC class was not registered in this classification (see annex 04: overlapping of 2013 classification and visual interpretation results).

Per fire occurrences

Identification and counting of the possible fire warnings from 2001 to 2017 were recorded using MODIS sensor data. Additionally, fire warnings on 2015 were isolated given the high incidence in that year. The results are summarized in Table 8:

Table 8 Visual interpretation results, total of detected fires warning from 2001 to 2017 and on 2015 per regency (in absolute numbers of warnings and relative proportions - p).

Regencies	Total of fire warnings	p (%)	Fire warnings from 2015	p (%)
Batang Hari	74	12	14	10
Bungo	62	10	16	11
Jambi	0	0	0	0
Kerinci	49	8	4	3
Merangin	86	14	9	6
Muaro Jambi	55	9	17	12
Sarolangun	86	14	29	21
Tanjung Jabung Barat	62	10	13	9
Tanjung Jabung Timur	62	10	22	16
Tebo	80	13	17	12

The incidence of forest or land fire events is evenly distributed in most of the different regencies. A total of 616 possible fire warnings were detected from 2000 to 2017. The fires, that have been identified per regency, ranged from 8 to 14 %. However, on 2015, 141 out of all the 616 possible warnings were detected (around 23 % in one out of eighteen years of analysis), the proportions went above or under this range. In Sarolangun and Tanjung Jabung Timur, the proportions were 21 and 16 % respectively, whereas, in Kerinci and Merangin, the proportions were 3 and 6 % respectively.

Per image acquisition year

As for the year of acquisition of the different satellite images, 2 % of the plots were classified with images from 2017, 59 % with images from 2016, 14 % with images from 2015, and 13 % with images from 2014. Finally, 11% of the plots used imagery from 2001 to 2013. Within this group, 49 plots were classified as secondary forests, 17 as natural areas, 16 as primary forests, and 12 as oil palm. Even though, the main idea was to ensure that most of the images were not older than 2013, when the last LC classification was implemented.

4.2. Image pre-processing and enhancement

For pre-processing activities, pan-sharpening technique was executed using PAN band of Landsat-8 satellite imagery, as a reference for increasing the spatial resolution of the rest of the bands (from 30 to 15 m spatial resolution). Figure 15 shows the effect of the change in Band 4 within an oil palm plantation. The new sub-divided pixels presented different shades of red, that increased the variety of possible DN that represent them.
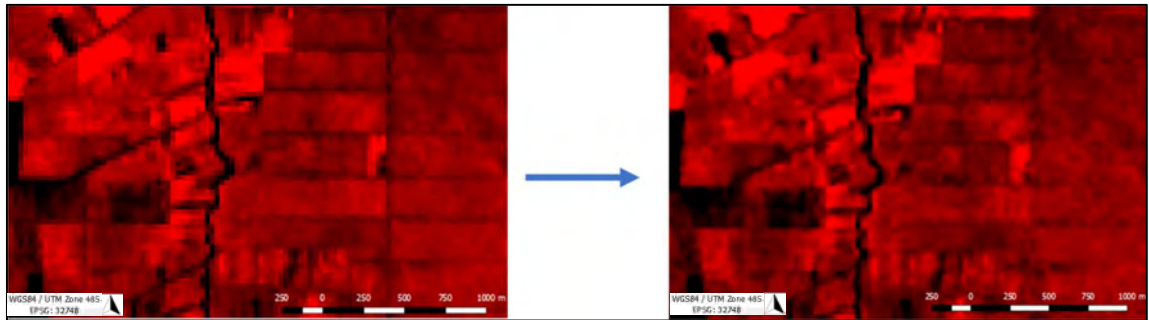

Figure 15 Pan-sharpening effect in an oil palm plantation (Lansat-8 Band 4). Produced from New Print Composer in QGIS. Coordinate System WGS84.

Once the spatial resolution of the bands was modified, image enhancement was executed using the PCA algorithm, that resulted in a new image with four components as shown in Figure 16. On the left, a multispectral image of 7 bands, expressed in natural colour, presents a plantation forest surrounded by oil palm plantations and water bodies; whereas on the right, the effect of the four components - PCA algorithm, exhibiting new colour patterns, is shown below.
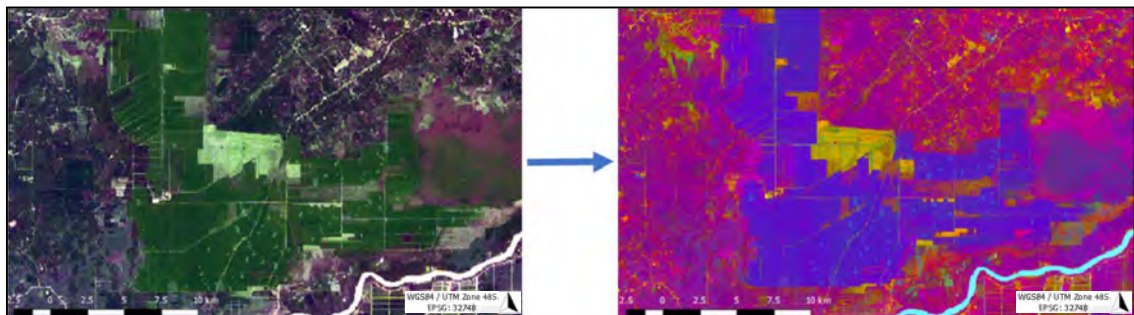

Figure 16 PCA effect showing a plantation forest and oil palm plantation classes (natural colour), and PCA image with four components. Produced from New Print Composer in QGIS. Coordinate System WGS84.

4.3. Assessment of reference data

The fieldwork was carried out in a range of three weeks in July of 2018. In summary, 1733 points were taken, 452 points for forest macro class, 424 for natural areas, 627 for

agricultural land, 22 for water bodies, 93 for urban areas, and 115 for others. Table 9 shows the allocation of points taken per LC class.

Table 9 Distribution of reference data taken from the field, expressed in units per LC classes and grouped into macro-classes.

Macro-class	LC Classes	Count
Forest	Primary forest	1
	Secondary forest	202
	Secondary swamp forest	122
	Plantation forest	116
	Bamboo	11
Natural areas	Shrub/bushland	106
	Shrub swamp	121
	Swamp	184
	Grassland	13
Agricultural land	Oil palm	255
	Rubber	122
	Dryland agriculture	79
	Fallow land	29
	Jungle rubber	19
	Mixed garden	12
	Orchard	29
	Paddy field	82
Water bodies	Water bodies	22
Urban areas	Urban areas	93
Others	Mining	26
	Open/bare land	55
	TOF	34
	TOTAL	1 733

Since the methodology consisted of taking points that can be visible for the user in the field, gathering primary forests (in drylands, swamps, and mangroves) was more difficult. To complete the missing LCs, visual interpretation plots were used as a new reference, with the plots that also coincided with the last LC map from 2013.

4.4. Classification and accuracy assessment

In order to assess the spectral signatures, two groups from the gathered points were randomly separated (training and validation data). Furthermore, two criteria were considered to produce spectral signatures: (1) to coincide with 2013 classification keys (ten LC classes indicated on page 20); and (2) Not to coincide with clouds or shadow in

the satellite image mosaic. Therefore, the final LC classes were: Primary forest, secondary forest, plantation forest, natural areas, dryland agriculture, oil palm plantation, rubber plantation, jungle rubber, water bodies, and urban areas. Hence, some of the LC classes from Figure 12 had to be either excluded or merged for the generation of spectral signatures.

Table 10 shows the final report for the classification.

Table 10 Supervised classification report, area and percentage per LC class.

LC Class	Area (km^2)	Percentage (%)
Primary forest	12 344	25.12
Secondary forest	9 546	19.42
Plantation forest	2 581	5.25
Natural areas	3 664	7.46
Agriculture	3 825	7.78
Oil palm	7 302	14.86
Rubber	5 045	10.26
Jungle rubber	3 714	7.56
Water	581	1.18
Urban areas	544	1.11
TOTAL	49 144	100.00

Per LC class

According to Table 10, primary forest occupied most of the extended area in the province with around 25.12 %, followed by secondary forest with 19.42 %. Furthermore, the agroindustry plantations: oil palm and rubber, occupied 14.86 and 10.26 % respectively. Natural areas, agriculture, and jungle rubber each had around 7 to 8 % of the province extension. Lower proportions were occupied by plantation forest (5.25 %), water bodies (1.18 %), and urban areas (1.11 %).

Comparing with 2013 classification, oil palm passed from 12.2 to 14.86 %, plantation forest from 4.6 % to 5.25 %, and others (that included urban areas and water bodies) from 3.8 % to 2.29 %, showing smooth changes. Both primary (25.12 %) and secondary forest (19.42 %) could have been over-classified. The two types of forests were allocated above the data from 2013 (16.8 % and 12.9 % respectively). Jungle rubber class (7.56 %) was also likely over-classified, from 1990 to 2013, its coverage did not get over 2 %.

Per macro-class

When the LC classes were grouped in macro-classes, the forest (including plantation forest) covered 49.79 % of the province, natural areas macro-class followed with 7.46 %, agricultural land had 40.46 %, and the rest was covered by water bodies and urban areas with the same proportions.

Map appearance

Figure 17 shows the updated land cover map for 2018, showing the 10 different LC classes, three for forests classes (green colour), one for natural areas (red colour), four for agriculture (yellow colour), one for water bodies (blue colour), and one for urban areas (light blue colour).
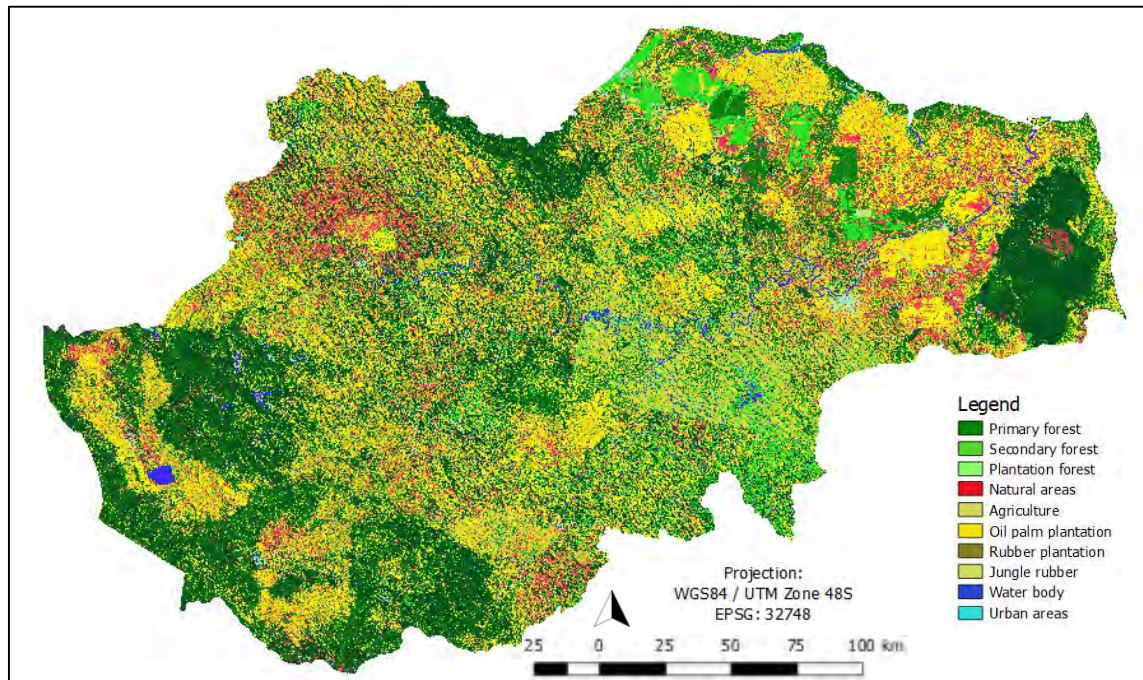
Figure 17 Land Cover map developed by supervised classification. Showing three LC classes related to forests in green shapes, one natural areas class in red shapes, four agricultural classes in yellow shapes, and water bodies and urban areas in blue shades. Produced from New Print Composer in QGIS. Coordinate System WGS84.

It is shown that the north-eastern area, that fits with Tanjung Jabung Barat, Tanjung Jabung Timur and part of Muaro Jambi (Figure 3), had a homogeneous pattern of classification. Likewise, the western area presented similar patterns, where the regencies of Kerinci and part of Merangin and Sarolangun are located. Meanwhile, the areas within Tebo, Bungo, and Batang Hari regencies (in the centre of the province) presented unclear areas in the LC map.

Between the two clear areas in the map, the coverage is dominated by primary, secondary, and plantation forests as well as oil palm and agriculture. Two zooming in of these areas into the map are shown in Figure 18 and Figure 19. The presence of agricultural crops in the eastern part and a river in the south of Figure 18 are clear in both: natural colour image and the classification. Likewise, in Figure 19, the presences of a lake at the centre, surrounded by agriculture and a further forest are strongly differentiated in the two features.
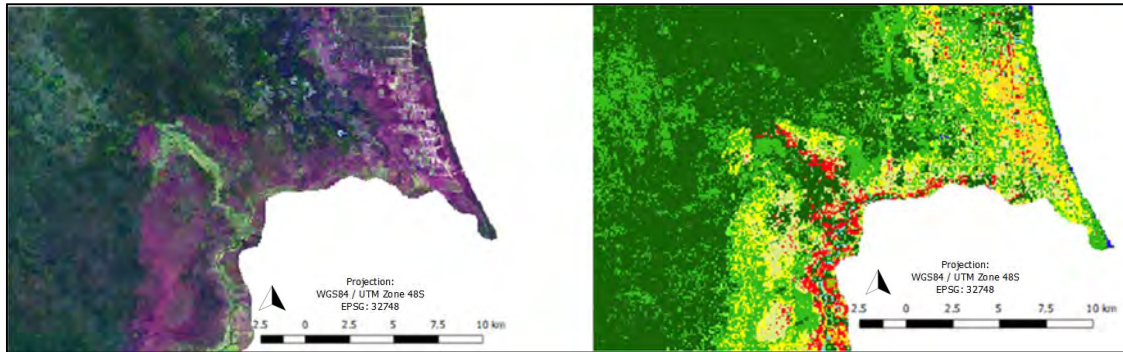
Figure 18 Left side natural colour for the southern part of Berbak national park / Right side Supervised classification. Produced from New Print Composer in QGIS. Coordinate System WGS84.
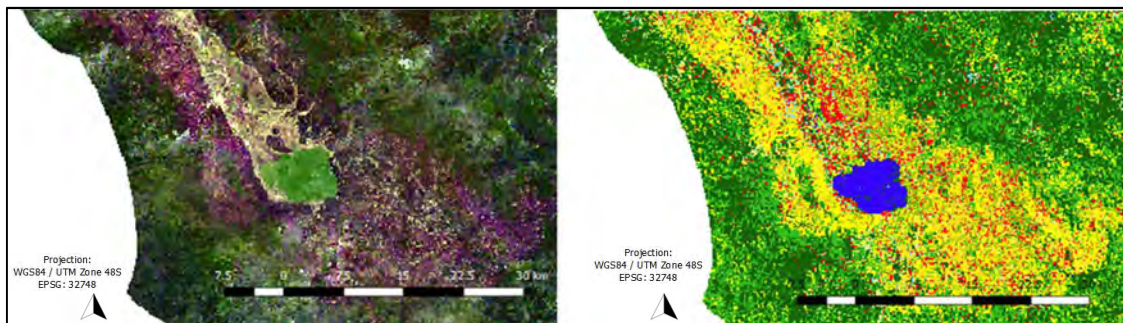

Figure 19 Left side natural colour for the central part of Kerinci national park / Right side Supervised classification. Produced from New Print Composer in QGIS. Coordinate System WGS84.

The third area, that was possible to distinguish a clear LC area is in the north-central side of Jambi (see Figure 17), where a green shade of the primary forest is found. All these three areas fall together in three of the national parks: Berbak in the east that preserves the swamp forest, Bukit Tigapuluh in the north, that preserves the lowland forest, and Kerinci Seblat, that protects the mountain forest in the western part of the province.

Heterogeneous patterns were observed in the resultant map for the central side of the province. These patterns arose from the former cloud masking and different colour shades observed in Figure 9. It was evident from Figure 20 that masking cloud stripes could have been misclassified, either for forest or oil palm plantations. In the upper right corner of

the same figure (for both features), a stripe of haze could have been misclassified for rubber plantation. The stripe is clearly visualized on location P125/R061 from Figure 7. However, LC classes such as water bodies and urban areas (left side of Figure 20) or natural areas (on the upper centre of the figure) could have been correctly classified.
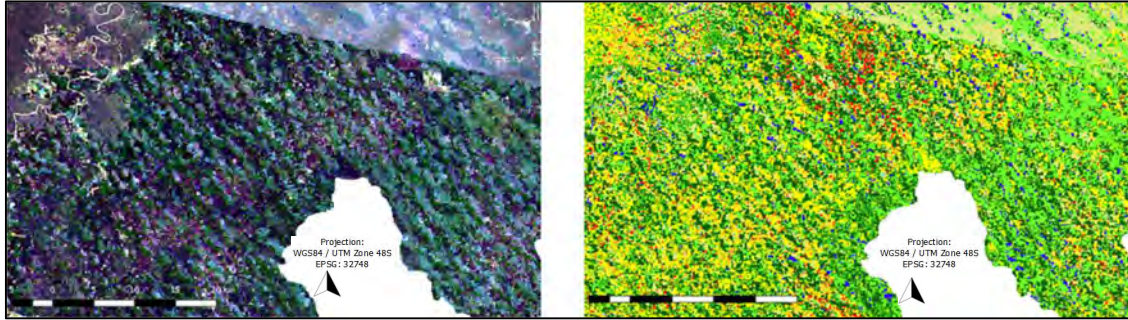

Figure 20 Left side Natural colour for the central-south side of Jambi / Right side Supervised classification. Produced from New Print Composer in QGIS. Coordinate System WGS84.

These clouds and haze shapes were also seen in the areas that were classified as agricultural lands in 2013 classification (mostly in the south of Jambi).

Accuracy assessment

The possible misclassifications can be better understood by analysing the confusion matrix in Table 11.

Table 11 Accuracy assessment results - Confusion matrix: ID key 1. Primary forest, 2. Secondary forest, 3. Plantation forest, 4. Natural areas, 5. Agriculture, 6. Oil palm, 7. Rubber plantation, 8. Water bodies, 9. Urban areas, 10. Jungle rubber.

	ID	1	2	3	4	5	6	7	8	9	10	Sum	PA (%)
						Classified							
Reference	1	**40**	6	2							1	49	81.6
	2	12	**10**		1	2	7	13		1	3	49	20.4
	3	7	12	**26**				4				49	53.1
	4	3	11		**6**	10	3	15		1		49	12.2
	5	2	1		2	**28**		7	3	5	1	49	57.1
	6	1	17		1	3	**20**	4			3	49	40.8
	7		8		16		8	**9**	2		6	49	18.4
	8			6					**43**			49	87.8
	9				3	14			3	**29**		49	59.2
	10		13		3	6		1			**26**	49	53.1
	Sum	65	78	34	32	63	38	53	51	36	40	416	
	UA (%)	61.5	12.8	76.5	18.8	44.4	52.6	17.0	84.3	80.6	65.0	OA	57.0

Table 11 shows the interactions between the training points and the assessment points. The overall accuracy (OA) of the map was 57 %. Highlighted numbers express the number of pixels that were correctly classified. To interpret this OA, first and foremost an assessment of the User Assessment (UA) is written, and furthermore, the presentation of Producer Assessment (PA) is detailed.

At user level (quality of the map), water bodies, urban areas, and plantation forests were the classes with the highest UA (higher than 75 %). In the case of plantation forests, some of their misclassified pixels were confused for water bodies. Furthermore, jungle rubber, primary forest, oil palm, and agriculture had lower UA (between 40 to 65 %) than the group explained above. The most problematic class in this group was agriculture, whose misclassified pixels represented more than 50 %. Finally, natural areas, rubber, and secondary forest had the lowest UA (lower than 20 %). It means that more than 80 % of their classified pixels could be incorrect, and according to the confusion matrix, the misclassified classes could be all the rest except water bodies. The worth mentioning case was secondary forests, whose most misclassifications were in plantation forest, oil palm and jungle rubber.

At the producer level (quality of the classification), water bodies and primary forest had the highest PA (higher than 80 %). In this case, more primary forest pixels from reference data were correctly classified, some of their confusion pixels came from the secondary forest, whereas water bodies had the highest accuracy value. Urban areas, agriculture, plantation forest, jungle rubber, and oil palm had lower PA (between 40 and 60 %). These classes had a regular distribution of incorrectly classified pixels based on the reference data, however, the secondary forest was the common class for all these misclassified pixels. In the case of oil palm, almost the same number of correctly and incorrectly classified pixels were reported in the confusion matrix. Secondary forest, rubber plantation, and natural areas had the lowest PA (lower or equal than 20 %), being natural areas class the one that showed much more misclassified pixels than the rest (mostly in rubber plantations, secondary forests, and agriculture).

5. Discussion

5.1 Sample based analysis
Per LC class and macro-class

Starting this analysis, it is important to note the presence of the "unclassified" LC class. "Unclassified" LC classes (see Table 5) are included in four macro-classes when only the macro-class level was identified in the plot. For instance, a plot could have been assigned into macro-class "agriculture land", but it was not possible to differentiate the LC class that could have fit in, either oil palm, dryland agriculture or rubber. This effect was originated from two factors: (1) cloud cover that blocks the land (Xiangsheng, Yonggang, and Anding 2011), and (2) low image resolution, that allows seeing the land but not clear enough to distinguish what is in there. However, for point (2), other factors are important to allow adequate interpretation of digital images, such as influence of atmosphere, object shadows, and others (Kovarik 2012). These points could have been classified as any other macro-class.

Moreover, an extra macro-class called "unclear" was included when neither macro-class nor LC class could be classified. Within these plots, cloud cover did not represent a significant problem in the classification, however, image resolution represented almost 8 % of the complete classification. According to Ramzi and Nedkov (2008), high image resolution is a key factor for extracting interpretation keys. This is one of the weaknesses of this methodology with regards to the software, the quality of some images was inadequate for specific areas, that the plot had been systematically positioned.

As for the comparison with the past classifications (Melati 2018), a tendency in the development of oil palm plantations with time in Jambi was found. This behaviour showed that oil palm LC has been relatively constant since the year 2000. Besides the observed sources, Global Forest Watch (2018) stated that in 2013/2014, oil palm plantation represented 12.9 % of Jambi province. The same stability could also be observed in primary forest. Moreover, primary forest plots were found in the same geographical area than the four national parks mentioned in the introduction of this document (see Figure 14). According to Table 7, Kerinci, Sarolangun, and Merangin are the regencies that contained more forest cover. Kerinci Seblat national park covers part of these regencies and contains large blocks of forests (Linkie et al. 2003).

For jungle rubber LC class, the value is lower than the ones from 2011 and 2013. This likely under-classification could have occurred because of the similarity between secondary forest and jungle rubber, that is a type of agricultural practice that uses rubber and other trees as the canopy coverage (Gouyon, de Foresta, and Levang 1993).

Regarding the likely misclassifications, secondary forest showed an unexpected value of 30.33 %, considering that this LC class had lower percentages in the previous years.

When comparing results from visual interpretation and 2013 classification, agricultural land values could have been under-classified, whereas rubber plantation values could have been over-classified. Besides likely explanations, within agricultural land macro-class, several LC classes were contained (see Table 7), including "unclassified" class, that represented more than 10% of this macro-class. Misclassifications could also be explained for this fact.

The most likely reason to explain the mentioned unexpected results is the over-classification of plots in secondary forest. Many of the rubber plantation plots could have been classified as secondary forest. It could have occurred because of the similarity of their visual patterns (key elements used as ancillary components to assign a class). In fact, an overlap exists between several secondary forest plots and the rubber plantations polygon from 2013 (annex 04).

According to this overlap, secondary forest and unclear plots were assigned where rubber plantation used to be located. Hence, considering that 30 to 40 years is the range that secondary forest can be produced from natural regeneration, in pastures or agricultural lands (Chazdon 2008), it is impossible that rubber plantations had turned into secondary forest in five years. This class was overclassified by mistake due to lack of experience and local knowledge of the study area. Even with ongoing digital processing techniques, it is worth mentioning the training of the human resource to gain skills (Prasad, Sinha, and Ranjan 2002). For the case of agricultural land in the overlap, 20 secondary forest plots could have been misclassified in this LC class.

A notable issue is the absence of plantation forest LC class in this classification. According to (Global Forest Watch 2018), around 5% of Jambi province is covered by plantation forests.

Per fire occurrences and regencies

The use of fire (slash and burn) is a traditional method for clearing and preparing areas for small-holder agriculture in Indonesia (Ketterings et al. 1999). Therefore, agricultural coverage could be related to forest warnings. In Kerinci and Merangin, where the higher forest and lowest agriculture classes were reported (see Table 7), fire warnings were lower than the rest of the regencies during 2015 (see Table 8). Another way around was the case of Tanjung Jabung Timur (one of the most important rice producers in Jambi according to Adam et al. (2013)), which reported the highest agriculture land coverage, and one of the highest values of fire warnings. It was shown that the fires warnings were more constant in the areas with higher agricultural lands areas.

Most of the fire hotspots from 2001 to 2014 occurred in secondary forest, grass, and shrubs LC classes in Jambi. According to Prasetyo et al. (2016), after fire events, they were converted into plantation forest (20.7 %), palm oil plantations (27 %), and smallholder or land community area (52.3 %). As for this classification "smallholder or land community" was classified as agriculture, this LC class and the regencies with the most incidences of fires warnings coincided in the north-eastern areas of Jambi (see Figure 14).

Per image acquisition year

Different years of satellite sources could have been another cause of misclassification. From the 1 009 selected images, 117 were from years before 2013. Even though the primary forest could have not been misclassified, secondary forest, natural areas, and oil palm could have. Not finding good temporal image sources is a common challenge in Jambi, for example, the study "Expansion of oil palm plantations and forest cover changes in Bungo and Merangin Districts, Jambi Province, Indonesia" (Tarigan, Sunarti, and Widyaliza 2015), stated that finding adequate satellite imagery for some particular years is not possible.

Recommendations for future integral classification

In summary, the main advantages of this technique were: (1) large availability of imagery resources, therefore, it was simple to avoid images with large areas of cloud cover, and overview surfaces from past years, (2) low cost technique, since it was performed by one user and no need to gather data from the field, and, (3) the possibility to identify fire

warnings. The main disadvantages were: (1) several images with low spatial resolution did not allow to correctly allocate a LC class, and (2) the necessity of experience and local knowledge was a limiting factor since this technique started before the fieldwork for supervised classification. Therefore, the further recommendations should be followed to improve the classification, using integrally visual interpretation and supervised classification.

Most of the images should be as recent as possible. Even when they are not the newest, all of them should be older than 2013 (when the last LC classification was done). Also, the skills and experience of the observer should be the best possible, therefore, even different conditions mentioned lines above, the LC will be assigned correctly to the appropriate class. Hence, the user must recognize all the classification keys for every LC class. Past classifications as shapefiles to overlay in the visual interpretation software should be used as ancillary elements. Finally, no plot should be classified as unclear class and plantation forest must be included. Classification keys from both techniques should be comparable.

Once all the plots are correctly classified and revised, they could be used as additional reference data for a further supervised classification.

5.2 Image pre-processing and enhancement

Pan-sharpening effect on one of the bands from the imagery is shown in Figure 15. The boundaries of the crops were slightly delineated and new colours were located within them. More digital information is presented for the image. On one hand, this fact is positive for visual interpretation since the new pattern facilitated the delineation of classes for the user. On the other hand, noise due to the heterogeneous components for further supervised classification technique could have been created in some areas for the rest of the bands (Inamdar et al. 2008). It could have occurred in the zones where several land cover classes were together.

Regarding image enhancement, using the PCA (Bayes) algorithm was useful in order to compress the most important data for the mosaic (Lillesand, Kiefer, and Chipman 2007), but also this algorithm was highly appreciated for size reduction. The image mosaic size was changed from 10 to 6 GB after image enhancement. This reduction was critical to continue with the classification, not only because of the enhancement itself but also

because the speed of processing was improved for classification. Even though SCP recommends to manipulate speed of processing (Congedo 2016), the computer had 32 MB RAM memory, that did not allow the processing of such a high sized mosaic. Hence, in order to classify an area using QGIS, either the computer should have had a higher memory RAM, or the image should have a lower size than 6 GB. Otherwise, software like Monteverdi 6.6 from Orfeo toolbox is recommended (Rao and Rajinikanth 2014).

5.3 Assessment of reference data

For efficient use of resources in the field, a good road shapefile, local knowledge from members of the EFForTS project in Jambi, and constant consultation with local leaders in the villages in the different visited communities were necessary to distinguish the best driving schedule.

Using the Trimble Juno 3B was an efficient technique for gathering multiple points a time as reference data for supervised classification. This device is nowadays operated for data collection and further integration within Geographic Position Systems - GPS (El Abbous 2012). During the fieldwork, it was possible to take 10 points for 3 different LC classes, by standing in a position in the road (station). Once the user had enough experience to manage the Trimble Juno 3B and to the laser device, the taken points could be located from a broad distance range of the user.

In order to gather the most and best quality points, stopping in an open and elevated area is recommended, more likely a small hill on the road or a log bridge that connects two land areas divided by a river. Otherwise, trees and shrubs could be obstacles for the user and consequently, only points too closed to each other, not so many of them, and likely from the same LC class would be collected.

Considering the long distances covered (see Figure 11), using a double traction car is recommended. An extra advantage is that standing up on the truck hopper to gain more height in relation to the ground level is possible, and therefore gathering more and better-quality points. Starting as early as possible and driving to the longest distance is also recommended. During this trip, the possible stations to gather the points were observed. Once the driver stopped at the farthest possible distance, the team went back to the base camp and stopped in the selected stations.

The best timeframe to work with the laser device was during the daylight hours. Working with a low incidence of light was not optimal. Another limiting factor was the rain, therefore during raining days, staying at the base camp and analysing information instead of driving to the field was the best option. Finally, when the stations were in dusty areas such as unsealed roads, the laser device did not work efficiently (Resource Supply LLC 2015). Even though the areas could be open like in a plantation forest, the dust could be considered as a point to gather by the laser device.

Table 9 shows the summary of points taken per class. Given that this methodology consisted of driving around and near the road matrix, it was not possible to be close enough to primary forest. Classes with more than 100 points were easier to gather and recognize, due to the way they were grouped into large areas, such as clusters of secondary forests and oil palm plantations. On the contrary, classes like bamboo, mixed garden or grassland were only found beside the roadside and not forming large clusters, therefore, fewer than 20 points were gathered. A special case occurred with jungle rubber class, which was neither beside the roadside nor easy to recognize from any station.

Recommendations for integrated classification

When it is possible, gathering more points, that contain agriculture LC from different kinds of crops, such as rice, coconut plantations, tee, and more is recommended. Since this LC class could be so heterogeneous, it is important to identify how much it could vary. Another critical LC class is jungle rubber, more points should be gathered since this class is commonly surrounded by secondary forest. Finally, a more reliable overall assessment will be produced.

Considering the stated conditions and recommendations, reference data should be obtained from two sources: field data from supervised classification technique, and the classified plots from the visual interpretation technique. Hence, both techniques will be implemented complementarily for one unique LC classification.

5.4 Classification and accuracy assessment

Comparing the results of the supervised classification (Table 10) and Melati's classification (Table 2), only oil palm, plantation forest, urban areas, and water bodies (the last two included in "others" in Melati's classification), followed a pattern along the

time. The distribution of plantation forest for the supervised classification (Figure 17) was as the same in this study as in the study of Melati (2018) (Figure 4). Besides them, the rest had quite unexpected distributions.

Per LC class and map appearance

As for comparing the supervised report with 2013 classification, it has been stated above that for the visual interpretation, at least primary forest could have been correctly classified. However, in the supervised classification, the two types of natural forests were over-classified. By analysing the LC map (Figure 17), primary and secondary forest have been classified around the four national parks, but also, irregular dispersions of these classes were found at the centre of the map. These likely misclassifications can also be noticed in the confusion matrix (Table 11), where secondary forest class had confused pixels with almost all the classes, except for water bodies and urban areas. Therefore, analysis with this classification could bring results that underestimate this class (Czaplewski 2003). It could explain why many past classified areas as agriculture or rubber plantations, have been located as secondary forest in this classification. Both secondary forest and rubber plantations were the classes that showed the lowest UA (see Table 11); the most misclassified pixels in the map could be represented by these two classes.

Jungle rubber was likely over-classified. In regular conditions, its similarity with secondary forest (Gouyon, de Foresta, and Levang 1993) could have been the cause of this effect. It was also visible in the confusion matrix, that jungle rubber class had confusions with rubber plantations, oil palm, and secondary forest.

However, an extra challenge for this classification was the quality of the cloud mask from GEE. Evenly distributions are shown in Figure 18 and Figure 19, whereas, unevenly features are exposed in Figure 20, where the cloud mask was overlaid. When comparing Figure 20 with the corresponding area from Figure 4, agricultural LC classes are not equally distributed. This fact evidenced the effect of a low-quality cloud mask in a supervised classification, considering such a big area. For large territories, such as Jambi, GEE cloud mask faces missing data due to cloud and shadows (Shelestov et al. 2017). A similar effect could have occurred with agriculture, rubber, and natural areas LC classes, that in these cases could have been sub-classified considering the classification from 2013. What apparently had occurred is that many of the pixels that could have contained

agriculture, rubber plantations, and natural areas, were classified as primary forest, secondary forest, and jungle rubber. The confusion matrix showed that most of the agriculture pixels were confused for rubber plantations, and consequently also with secondary forest.

The cloud cover problem is a constant challenge in Indonesia, as it was said before, finding a seasonal cloud-free imagery is impossible (Gastellu-Etchegorry 1988). For future classifications, using cloud masking techniques, that include more sophisticated technologies would definitely go a long way in providing a solution to this challenge. Technologies such as regression trees to predict the values of the land covered by clouds and shadows, and applying different time scenes as references (Helmer and Ruefenacht 2005). For instance, based-available-pixel (BAP) composites have already been used with Landsat imagery to cover the whole country of Canada (White et al. 2014).

Nevertheless, not all the areas in the map were likely misclassified. As it can be seen, Figure 18 showed a side of Berbak national park, agricultural land, natural areas, and a river flowing in north to south direction; and Figure 19 showed a part of Kerinci Seblat national park with the same LC classes and a lake in the centre. Hence, performing the classification either per regency or sub-areas such as basins would be ideal, considering the ones without a relatively high cloud cover. The classification of the Harapan forest in the south of Jambi province in 2013 (Melati 2018) and the Batang Hari basin in 2017 (Utami, Sapei, and Apip 2017) were already successfully done under supervised classification techniques.

Cloud cover effect can also be influenced by land and forest fires, according to Table 8, fire warnings were registered every year in Indonesia. Large smudges moving diagonally across the image represents smoke from fire (NASA Goddard Space Flight Center 2015), as could be seen in Figure 17. Most of the regions with less cloud cover were found in more forested areas and fewer agriculture lands and natural areas. This could have been since areas with a majority cover for agriculture are mostly dominated by land and forest fires, therefore, would have problems with dense cloud covers as seen in Figure 20.

Per macro-class

When overlaying the distribution of macro-classes classified under visual interpretation (Figure 14) with the supervised classification map (Figure 17), 37 out of 85 unclear points were allocated to the centre of the map, where the cloud problems had been detected (see

annex 05: overlapping of supervised classification and visual interpretation plots). A remarkable limitation of Landsat imagery in the humid tropics is the cloud cover and the consequent low quality for surface observations (Hansen et al. 2013). Urban areas and water bodies coincided and made sense between both classifications. Hence, urban areas were distributed between Jambi city and some settlements dispersed in the province, and water bodies around Batang Hari river and the lake in the western part of the province. Macro-class agriculture plots were mostly spread out on the eastern part of Jambi, while, according to the supervised classification, it was evenly and slightly distributed around the whole province. In the case of the macro-class forest, both classifications showed a broad distribution within Jambi province.

In comparison of both classifications, one of the weaknesses of the supervised classification was the absence of the macro-class "others". Same classification schemes should be used to compare classifications (C. Li et al. 2014). Given that it was necessary to reduce the number of classes, LCs such as mining and bare lands were classified as urban or natural areas, even though they could have had different spectral signatures (C. Li et al. 2014); whereas TOF as forests.

Recommendations for integrated classification

Summarising, the main advantages of supervised classification, as is stated in Table 1, were: (1) area estimation is more accurate than visual interpretation, and (2) Multi-spectral analysis is possible, therefore, more information can be considered for the classification. The main disadvantages found in this study were: (1) low quality cloud cover, that did not allow allocating LC classes correctly, and (2) classification keys from two techniques were different, hence, comparison was inefficient. Therefore, the following recommendations should be followed to perform an integrated classification:

The satellite image mosaic that covers the study area should be correctly prepared to avoid the previously mentioned problems. This mosaic should be from the same year than the set of imagery used for visual interpretation classification. In order to obtain the best image pixel by pixel, performing the cloud compositing algorithms using temporal series of images, is proposed. After this process, the effect of pan-sharpening could be evaluated, whether it is necessary to improve the spatial resolution or not, since for this study, it was use for visual proposes. Finally, PCA technique should be performed to

enhance and to reduce the size of the image. Classification and accuracy assessment should be executed likewise in this study.

Another option to improve the quality of the classification (expressed in the accuracy assessment), is to isolate the regencies and performed a supervised classification. In that case, the reference data could come directly from the classified plots from visual interpretation. These plots should have fewer distances between each other (less than 7 km) in order to cover more possible LC classes. Based on this method, isolated regencies such as Kerinci or the southern part or Sarolangun could be covered and fieldwork could not be necessary. Therefore, costs and time would be saved.

6. Conclusion

Performing separately LC classifications for Jambi province, using visual interpretation and supervised classification techniques, two different reports were produced. Expected and unexpected results were found and could be explained due to the advantages and disadvantages of both techniques.

For visual interpretation technique, a set of multi-temporal imagery sources from different satellites, the tool to detect fire warnings, and being a low-cost technique were their main advantages. Whereas, their main disadvantages were that this classification was limited to the user's experience and local knowledge, whereas several old digital imageries, that did not fit with the Landsat-8 image mosaic for supervised classification, were used. For supervised classification technique, the main advantage is, theoretically, its level of accuracy in comparison to visual interpretation. However, for this study, a large cloud cover in the mosaic, and heterogeneous classification keys between the two techniques were the disadvantages, that did not allow higher accuracies than the reported ones.

In order to produce an integral and updated LC classification in Jambi province, the pathway is as follows:

A new visual interpretation classification needs to be generated, following the same methodology explained in this research. The selected image per plot must be as recent as possible (most likely from 2018). When the image is unclear, past classifications can be used as ancillary elements. Each classified plot will represent a point for reference data for supervised classification.

Furthermore, when using more advanced compositing techniques with 2018 imagery, a free-cloud cover Landsat-8 satellite image mosaic should be produced. Pre-processing and image enhancement should be executed in the mosaic. Thus, reference data will be selected from two sources: (1) fieldwork points according to the final classification key; and (2) classified plots from visual interpretation to cover the whole province.

Once the reference data is divided into training and validation data, the classification will be performed. An accuracy assessment will be analysed to confirm the quality of the map.

7. References

Adam, Husin, Robiyanto H Susanto, Benyamin Lakitan, Ardiyan Saptawan, and M Yazid. 2013. 'The Problems and Constraints in Managing Tidal Swamp Land for Sustainable Food Crop Farming (A Case Study of Trasmigration Area of Tanjung Jabung Timur Regency, Jambi Province, Indonesia)'. In , 57:6. Singapore: IPCBEE.

Arunarwati Margono, Belinda, Svetlana Turubanova, Ilona Zhuravleva, Peter Potapov, Alexandra Tyukavina, Alessandro Baccini, Scott Goetz, and Matthew C. Hansen. 2012. 'Mapping and Monitoring Deforestation and Forest Degradation in Sumatra (Indonesia) Using Landsat Time Series Data Sets from 1990 to 2010'. Environmental Research Letters 7 (September): 034010. https://doi.org/10.1088/1748-9326/7/3/034010.

Australian Department of Agriculture and Water Resources. 2017. 'Definitions for Land Use Management'. 2017. http://www.agriculture.gov.au:80/abares/aclump/definitions.

Badan Pusak Statistik. 2010. 'Sensus Penduduk 2010 - Provinsi Jambi'. BPS. 2010. http://sp2010.bps.go.id/index.php/site?id=15&wilayah=Jambi.

Barber, A. J., M. J. Crow, and J. S. Milsom. 2005. Sumatra: Geology, Resources and Tectonic Evolution. London: Geological Society of London.

Belgiu, Mariana, and Lucian Drăguţ. 2016. 'Random Forest in Remote Sensing: A Review of Applications and Future Directions'. ISPRS Journal of Photogrammetry and Remote Sensing 114 (April): 24–31. https://doi.org/10.1016/j.isprsjprs.2016.01.011.

Bontemps, S., P. Defourny, J. Radoux, E. Van Bogaert, C. Lamarche, F. Achard, P. Mayaux, et al. 2013. 'Consistent Global Land Cover Maps For Climate Modelling Communities: Current Achievements Of The ESA' Land Cover CCI'. In , 722:62. http://adsabs.harvard.edu/abs/2013ESASP.722E..62B.

Budiwati, Tuti, Wiwiek Setyawati, and Dyah Aries Tanti. 2016. 'Chemical Characteristics of Rainwater in Sumatera, Indonesia, during 2001–2010'. Research article. International Journal of Atmospheric Sciences. 2016. https://doi.org/10.1155/2016/1876046.

Chazdon, Robin L. 2008. 'Beyond Deforestation: Restoring Forests and Ecosystem Services on Degraded Lands'. Science 320 (5882): 1458–60. https://doi.org/10.1126/science.1155365.

Climate-Data.org. 2018. 'Climate in Jambi'. CLIMATE-DATA.ORG. 2018. https://en.climate-data.org/location/972263/.

Congedo, Luca. 2016. 'Semi-Automatic Classification Plugin Documentation. Release 6.0.1.1'. https://doi.org/10.13140/rg.2.2.29474.02242/1.

Czaplewski, Raymond L. 2003. 'Accuracy Assessment of Maps of Forest Condition'. In Remote Sensing of Forest Environments, edited by Michael A. Wulder and Steven E. Franklin, 115–40. Boston, MA: Springer US. https://doi.org/10.1007/978-1-4615-0306-4_5.

Dewanti Dimyati, Ratih, Projo Danoedoro, Hartono Hartono, and Kustiyo Kustiyo. 2018. 'A Minimum Cloud Cover Mosaic Image Model of the Operational Land Imager Landsat-8 Multitemporal Data Using Tile Based'. International Journal of Electrical and Computer Engineering (IJECE) 8 (1): 360. https://doi.org/10.11591/ijece.v8i1.pp360-371.

Di Gregorio, Antonio. 2016. Land Cover Classification System - Classification Concepts Software Version 3. Rome.

Di Gregorio, Antonio, and Louisa J. M. Jansen. 2000. 'LAND COVER CLASSIFICATION SYSTEM'. 2000. http://www.fao.org/docrep/003/x0596e/X0596e00.htm#P-1_0.

Ehlers, Manfred, Sascha Klonus, Pär Johan Åstrand, and Pablo Rosso. 2010. 'Multi-Sensor Image Fusion for Pansharpening in Remote Sensing'. International Journal of Image and Data Fusion 1 (1): 25–45. https://doi.org/10.1080/19479830903561985.

El Abbous, Abdellah. 2012. 'GPS Signal Accuracy and Coverage Analysis Platform: Application to Trimble Juno SB Receiver'. International Journal of Information and Network Security (IJINS) 1 (2). https://doi.org/10.11591/ijins.v1i2.532.

Escrig, H., F. J. Batlles, J. Alonso, F. M. Baena, J. L. Bosch, I. B. Salbidegoitia, and J. I. Burgaleta. 2013. 'Cloud Detection, Classification and Motion Estimation Using Geostationary Satellite Imagery for Cloud Cover Forecast'. Energy 55 (June): 853–59. https://doi.org/10.1016/j.energy.2013.01.054.

Estornell, Javier, M. Teresa Sebastiá, and Jesus Mengual. 2013. 'Principal Component Analysis Applied to Remote Sensing'. Modelling in Science Education and Learning, 2013.

FAO. 2016a. Global Forest Resources Assessment 2015. How are the World's Forests Changing? Second edition. Rome, Italy: FAO. www.fao.org/3/i4793e/I4793E.pdf.

———. 2016b. Map Accuracy Assessment and Area Estimation: A Practical Guide. National Forest Monitoring Assessment Working Paper, No.46/E. Roma. https://www.unredd.net/announcements-and-news/2351-new-fao-guide-to-map-accuracy-assessment-and-area-estimation-for-forest-monitoring.html.

———. 2018. 'Open Foris Software Tool'. Forest Monitoring and Assessment. 2018. http://www.fao.org/forestry/fma/openforis/en/.

Fauvel, Mathieu. 2008. 'Spectral and Spatial Methods for the Classification of Urban Remote Sensing Data'. Doctoral Thesis, Institut National Polytechnique de Grenoble - INPG; Université d'Islande, 2007.

Fonji, Simon Foteck, and Gregory N Taff. 2014. 'Using Satellite Data to Monitor Land-Use Land-Cover Change in North-Eastern Latvia'. SpringerPlus 3 (January). https://doi.org/10.1186/2193-1801-3-61.

Gastellu-Etchegorry, J. P. 1988. 'Cloud Cover Distribution in Indonesia'. International Journal of Remote Sensing 9 (7): 1267–76. https://doi.org/10.1080/01431168808954934.

Gibbs, H. K., A. S. Ruesch, F. Achard, M. K. Clayton, P. Holmgren, N. Ramankutty, and J. A. Foley. 2010. 'Tropical Forests Were the Primary Sources of New Agricultural Land in the 1980s and 1990s'. Proceedings of the National Academy of Sciences of the United States of America 107 (38): 16732–37. https://doi.org/10.1073/pnas.0910275107.

Giglio, Louis, Jacques Descloitres, Christopher O. Justice, and Yoram J. Kaufman. 2003. 'An Enhanced Contextual Fire Detection Algorithm for MODIS'. Remote Sensing of Environment 87 (2–3): 273–82. https://doi.org/10.1016/S0034-4257(03)00184-6.

Giglio, Louis, Wilfrid Schroeder, and Christopher O. Justice. 2016. 'The Collection 6 MODIS Active Fire Detection Algorithm and Fire Products'. Remote Sensing of Environment 178 (June): 31–41. https://doi.org/10.1016/j.rse.2016.02.054.

Global Forest Watch. 2018. 'Tree Cover Loss in Jambi, Indonesia'. December 2018. https://www.globalforestwatch.org/dashboards/country/IDN/8?category=land-cover&show_newsletter=true&widget=treeCoverLocated.

Golmehr, E. 2009. 'Current Application of Remote Sensing Techniques in Land Use Mapping: A Case Study of Northern Parts of Kolhapur District, India'. Journal of Applied Sciences and Environmental Management 13 (4). https://doi.org/10.4314/jasem.v13i4.55389.

Gouyon, A., H. de Foresta, and P. Levang. 1993. 'Does "Jungle Rubber" Deserve Its Name? An Analysis of Rubber Agroforestry Systems in Southeast Sumatra'. Agroforestry Systems 22 (3): 181–206. https://doi.org/10.1007/BF00705233.

Gupta, Ravi P., Reet K. Tiwari, Varinder Saini, and Neeraj Srivastava. 2013. 'A Simplified Approach for Interpreting Principal Component Images'. Advances in Remote Sensing 02 (02): 111–19. https://doi.org/10.4236/ars.2013.22015.

Hansen, M. C., P. V. Potapov, R. Moore, M. Hancher, S. A. Turubanova, A. Tyukavina, D. Thau, et al. 2013. 'High-Resolution Global Maps of 21st-Century Forest Cover Change'. Science 342 (6160): 850–53. https://doi.org/10.1126/science.1244693.

Helmer, E. H., and B. Ruefenacht. 2005. 'Cloud-Free Satellite Image Mosaics with Regression Trees and Histogram Matching'. Photogrammetric Engineering and Remote Sensing. http://agris.fao.org/agris-search/search.do?recordID=US201301833948.

Henebry, Geoffrey M. 2014. 'Advantages of Principal Components Analysis for Land Cover Segmentation from SAR Image Series.' ESA Earthnet Online - European Space Agency. 2014. http://earth.esa.int/workshops/ers97/papers/henebry3/index.html.

Heriyanto, Eko, Lailan Syaufina, and Mohamad Sobri. 2015. 'Forecasting Simulation of Smoke Dispersion from Forest and Land Fires in Indonesia'. Procedia Environmental Sciences 24: 111–19. https://doi.org/10.1016/j.proenv.2015.03.015.

Inamdar, Anand K., Andrew French, Simon Hook, Greg Vaughan, and William Luckett. 2008. 'Land Surface Temperature Retrieval at High Spatial and Temporal Resolutions over the Southwestern United States'. Journal of Geophysical Research: Atmospheres 113 (D7). https://doi.org/10.1029/2007JD009048.

Johnson, Brian. 2014. 'Effects of Pansharpening on Vegetation Indices'. ISPRS International Journal of Geo-Information 3 (2): 507–22. https://doi.org/10.3390/ijgi3020507.

Justice, C. O, J. R. G Townshend, E. F Vermote, E Masuoka, R. E Wolfe, N Saleous, D. P Roy, and J. T Morisette. 2002. 'An Overview of MODIS Land Data Processing and Product Status'. Remote Sensing of Environment, The Moderate Resolution Imaging Spectroradiometer (MODIS): a new generation of Land Surface Monitoring, 83 (1): 3–15. https://doi.org/10.1016/S0034-4257(02)00084-6.

Ketterings, Quirine M, Titus Tri Wibowo, Meine van Noordwijk, and Eric Penot. 1999. 'Farmers' Perspectives on Slash-and-Burn as a Land Clearing Method for Small-Scale Rubber Producers in Sepunggur, Jambi Province, Sumatra, Indonesia'. Forest Ecology and Management 120 (1–3): 157–69. https://doi.org/10.1016/S0378-1127(98)00532-5.

Khan Rahaman, Quazi Hassan, and M. Ahmed. 2017. 'Pan-Sharpening of Landsat-8 Images and Its Application in Calculating Vegetation Greenness and Canopy Water Contents'. ISPRS International Journal of Geo-Information 6 (6): 168. https://doi.org/10.3390/ijgi6060168.

Kim, Cheolmin. 2016. 'Land Use Classification and Land Use Change Analysis Using Satellite Images in Lombok Island, Indonesia'. Forest Science and Technology 12 (4): 183–91. https://doi.org/10.1080/21580103.2016.1147498.

Kovarik, Vladimir. 2012. 'Effects and Limitations of Spatial Resolution of Imagery for Imagery Intelligence'. In. Bratislava, Slovakia. https://www.researchgate.net/publication/266364885_Effects_and_limitations_of_spatial_resolution_of_imagery_for_imagery_intelligence.

Laben, Craig A., and Bernard V. Brower. 2000. Process for enhancing the spatial resolution of multispectral imagery using pan-sharpening. United States US6011875A, filed 29 April 1998, and issued 4 January 2000. https://patents.google.com/patent/US6011875A/en.

Lam, Nina Siu-Ngan. 2008. 'Methodologies for Mapping Land Cover/Land Use and Its Change'. In Advances in Land Remote Sensing, 341–67. Springer, Dordrecht. https://doi.org/10.1007/978-1-4020-6450-0_13.

Laumonier, Yves. 1997. The Vegetation and Physiography of Sumatra. Geobotany. Springer Netherlands. //www.springer.com/gp/book/9780792337614.

Laumonier, Yves, Yumiko Uryu, Michael Stüwe, Arif Budiman, Budi Setiabudi, and Oki Hadian. 2010. 'Eco-Floristic Sectors and Deforestation Threats in Sumatra: Identifying New Conservation Area Network Priorities for Ecosystem-Based Land Use Planning'. Biodiversity and Conservation 19 (4): 1153–74. https://doi.org/10.1007/s10531-010-9784-2.

Li, Congcong, Jie Wang, Lei Wang, Luanyun Hu, and Peng Gong. 2014. 'Comparison of Classification Algorithms and Training Sample Sizes in Urban Land Classification with Landsat Thematic Mapper Imagery'. Remote Sensing 6 (2): 964–83. https://doi.org/10.3390/rs6020964.

Li, Qianwen, Zhihua Wei, and Cairong Zhao. 2017. 'Optimized Automatic Seeded Region Growing Algorithm with Application to ROI Extraction'. International Journal of Image and Graphics 17 (04): 1750024. https://doi.org/10.1142/S0219467817500243.

Lillesand, Thomas, Ralph W. Kiefer, and Jonathan Chipman. 2007. Remote Sensing and Image Interpretation. 6 edition. Hoboken, NJ: Wiley.

Linkie, Matthew, Deborah J. Martyr, Jeremy Holden, Achmad Yanuar, Alip T. Hartana, Jito Sugardjito, and Nigel Leader-Williams. 2003. 'Habitat Destruction and Poaching Threaten the Sumatran Tiger in Kerinci Seblat National Park, Sumatra'. Oryx 37 (01). https://doi.org/10.1017/S0030605303000103.

Magdon, Paul, Hans Fuchs, Nils Nölke, and Christoph Kleinn. 2017. 'Classification Methods in Remote Sensing - Part 1 -'. Georg August Universität Göttingen. //columbiacollege-ca.libguides.com/apa/notes.

Margono, Belinda Arunarwati, Ahmad Basyirudin Usman, Budiharto, and Ruandha Agung Sugardiman. 2016. 'Indonesia's Forest Resource Monitoring'. Indonesian Journal of Geography 48 (1): 7–20. https://doi.org/10.22146/ijg.12496.

Melati, Dian Nuraini. 2018. 'The Use of Remote Sensing Data to Monitor Land Use Systems and Forest Variables of the Tropical Rainforest Landscape under Transformation in Jambi Province, Sumatra, Indonesia'. Göttingen: Georg August Universität Göttingen. https://ediss.uni-goettingen.de/handle/11858/00-1735-0000-002E-E323-E.

Mendoza, Guillermo, Giulio Marchi, Mayumi Quintos-Natividad, Mark de Claro, Bonifacio Rabang, Idelfonso Quilloy, Danilo Mollicone, Adia Bey, Alfonso SanchesPaus-Diaz, and Nilda Patiga. 2015. 'Publication - USING COLLECT EARTH TO ASSESS AND MONITOR LAND USE CHANGE IN SELECTED

REGIONS OF THE PHILIPPINES'. Asian Association on Remote Sensing. 2015. http://a-a-r-s.org/acrs/index.php/acrs/acrs-overview/proceedings-1?view=publication&task=show&id=1717.

Moore, R. T., and M. C. Hansen. 2011. 'Google Earth Engine: A New Cloud-Computing Platform for Global-Scale Earth Observation Data and Analysis'. AGU Fall Meeting Abstracts 43 (December): IN43C-02.

NASA Goddard Space Flight Center. 2015. 'Smoke and Fires in Sumatra'. Text.Article. 11 September 2015. https://earthobservatory.nasa.gov/images/86596/smoke-and-fires-in-sumatra.

Noordwijk, Meine van, Pablo Pacheco, Maja Slingerland, Sonya Dewi, and Ni'matul khasanah. 2017. 'Palm Oil Expansion in Tropical Forest Margins or Sustainability of Production? Focal Issues of Regulations and Private Standards'. World Agroforestry Centre.

Pal, M. 2005. 'Random Forest Classifier for Remote Sensing Classification'. International Journal of Remote Sensing 26 (1): 217–22. https://doi.org/10.1080/01431160412331269698.

Perbatakusuma, E.A., M. Ridwansyah, A Akiefnawati, R Widolo, W Kurniawan, D Primadona, I. Andrian, D. Lindawati, Alfiansyah, and M. Sakti. 2012. 'STRATEGI DAN RENCANA AKSI REDD+ PROVINSI JAMBI 2012 – 2032. DOKUMEN RISALAH EKSEKUTIF'.

Prasad, R., A. K. Sinha, and K. R. Ranjan. 2002. 'Visual Interpretation of FCC Image for Land Use and Land Cover Mapping: An Expert System Approach'. In Proceedings of the 41st SICE Annual Conference. SICE 2002., 4:2093–98 vol.4. https://doi.org/10.1109/SICE.2002.1195718.

Prasetyo, Lilik Budi, Arya H. Dharmawan, Fredian T. Nasdian, and S. Ramdhoni. 2016. 'Historical Forest Fire Occurrence Analysis in Jambi Province During the Period of 2000 – 2015: Its Distribution & Land Cover Trajectories'. Procedia Environmental Sciences 33: 450–59. https://doi.org/10.1016/j.proenv.2016.03.096.

QGIS. 2016. 'Welcome to the QGIS Project!' 2016. https://www.qgis.org/en/site/.

Ramzi, Ahmed, and Roumen Nedkov. 2008. 'CONSISTENT GLOBAL LAND COVER MAPS FOR CLIMATE MODELLING COMMUNITIES: CURRENT ACHIEVEMENTS OF THE ESA' LAND COVER CCI'. In, 102–5. Varna, Bulgaria. https://www.researchgate.net/publication/304788651_CONSISTENT_GLOBAL _LAND_COVER_MAPS_FOR_CLIMATE_MODELLING_COMMUNITIES_ CURRENT_ACHIEVEMENTS_OF_THE_ESA%27_LAND_COVER_CCI.

Rao, Tarun, and T.V. Rajinikanth. 2014. 'Supervised Classification of Remote Sensed Data Using Support Vector Machine | Request PDF'. Global Journal of Computer Science and Technology: Software and Data Engineering 14 (1): 71–76.

Resource Supply LLC. 2015. 'Using a Laser Rangefinder in Fog'.

Richards, John A. 2013. Remote Sensing Digital Image Analysis: An Introduction. 5th ed. Berlin Heidelberg: Springer-Verlag. //www.springer.com/gp/book/9783642300615.

Rijal, Syamsu, M. Buce Saleh, Nengah Surati Jaya, and Tatang Tiryana. 2016. 'Deforestation Profile of Regency Level in Sumatra'. International Journal of Sciences: Basic and Applied Research (IJSBAR) ISSN 2307-4531 25 (2): 385–402.

Rodarmel, Craig, and Jie Shan. 2002. 'Principal Component Analysis for Hyperspectral Image Classification' 62 (2): 9.
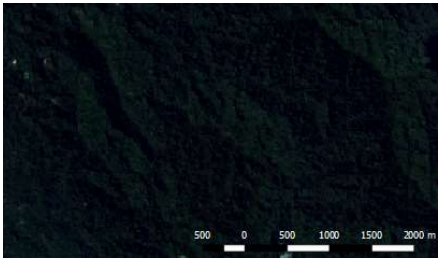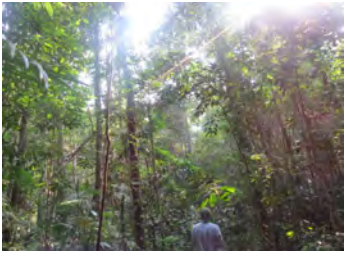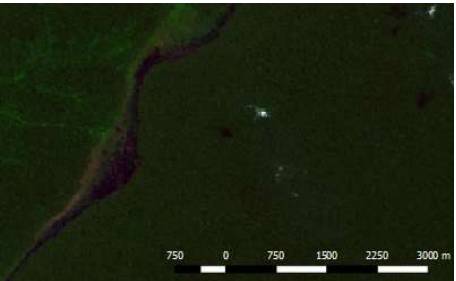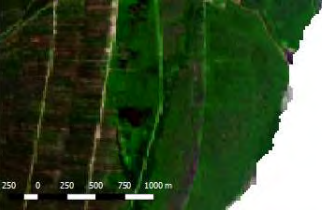
Schmidt, F. H., and J. H. A. Ferguson. 1951. 'Rainfall Types Based on Wet and Dry Period Ratios for Indonesia with Western New Guinea'. Verhandelingen, Djawatan Meteorologi Dan Geofisik, Djakarta. 4 September 1951. https://eurekamag.com/research/013/805/013805956.php.

Shelestov, Andrii, Mykola Lavreniuk, Nataliia Kussul, Alexei Novikov, and Sergii Skakun. 2017. 'Exploring Google Earth Engine Platform for Big Data Processing: Classification of Multi-Temporal Satellite Imagery for Crop Mapping'. Frontiers in Earth Science 5. https://doi.org/10.3389/feart.2017.00017.

Summer, H., and C. Nordman. 2008. 'Accuracy Assessment: Abraham Lincoln Birthplace National Historic Site'. Durham, North Carolina: NatureServe.

Syaufina, Lailan, Imas Sukaesih Sitanggang, and Lusi Maulana Erman. 2016. 'Challenges in Satellite-Based Research on Forest and Land Fires in Indonesia: Frequent Item Set Approach'. Procedia Environmental Sciences 33: 324–31. https://doi.org/10.1016/j.proenv.2016.03.083.

Tarigan, Suria Darma, Sunarti, and Susi Widyaliza. 2015. 'Expansion of Oil Palm Plantations and Forest Cover Changes in Bungo and Merangin Districts, Jambi Province, Indonesia'. Procedia Environmental Sciences, The 1st International Symposium on LAPAN-IPB Satellite (LISAT) for Food Security and Environmental Monitoring, 24 (January): 199–205. https://doi.org/10.1016/j.proenv.2015.03.026.

The World Bank. 2016. 'The Cost of Fire: An Economic Analysis of Indonesia's 2015 Fire Crisis'. 103668. The World Bank. http://documents.worldbank.org/curated/en/776101467990969768/The-cost-of-fire-an-economic-analysis-of-Indonesia-s-2015-fire-crisis.

US Department of Commerce, National Oceanic and Atmospheric Administration. 2017. 'What Is the Difference between Land Cover and Land Use?' 2017. https://oceanservice.noaa.gov/facts/lclu.html.

USGS. 2018a. 'EarthExplorer - Home'. 2018. https://earthexplorer.usgs.gov/.

———. 2018b. 'Landsat 8 | Landsat Missions'. USGS Science for a Changing World. 2018. https://landsat.usgs.gov/landsat-8.

Utami, Nurya, Asep Sapei, and Apip. 2017. 'Land Use Change Assessment and Its Demand Projection in Batanghari River Basin, Sumatera, Indonesia'. LIMNOTEK Perairan Darat Tropis Di Indonesia 24 (2): 52–60.

Verstappen, H. Theodoor, Koninklijk Nederlands Aardrijkskundig Genootschap, International Institute for Aerial Survey, and Earth Sciences. 1973. A Geomorphological Reconnaissance of Sumatra and Adjacent Islands (Indonesia). Groningen: Wolters-Noordhoff. https://trove.nla.gov.au/version/26028469.

Villamor, Grace B., Quang Bao Le, Utkur Djanibekov, Meine van Noordwijk, and Paul L. G. Vlek. 2014. 'Biodiversity in Rubber Agroforests, Carbon Emissions, and Rural Livelihoods: An Agent-Based Model of Land-Use Dynamics in Lowland Sumatra'. Environmental Modelling & Software 61 (November): 151–65. https://doi.org/10.1016/j.envsoft.2014.07.013.

Wang, Zhipeng, J. Scott Tyo, and Majeed M. Hayat. 2007. 'Data Interpretation for Spectral Sensors with Correlated Bands'. JOSA A 24 (9): 2864–70. https://doi.org/10.1364/JOSAA.24.002864.

Warsi.org. 2012. 'Distribution of Indigenous Groups in Jambi Province'. https://www.researchgate.net/publication/323572552_CHALLENGES_AND_RESILIENCES_Architecture_of_Semi-Nomadic_%27Orang_Rimba%27_in_the_Bukit_Duabelas_National_Park_Jambi/figures.
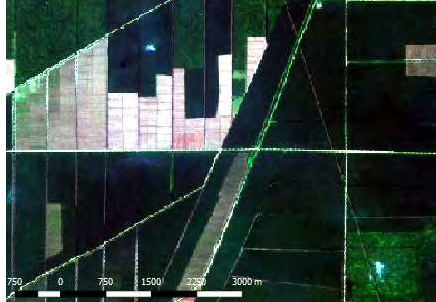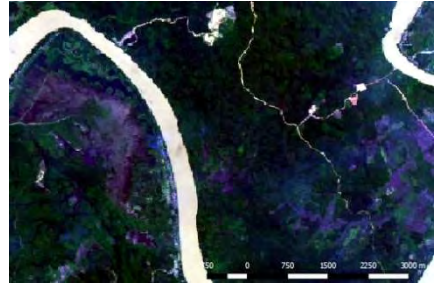
White, J. C., M. A. Wulder, G. W. Hobart, J. E. Luther, T. Hermosilla, P. Griffiths, N. C. Coops, et al. 2014. 'Pixel-Based Image Compositing for Large-Area Dense Time Series Applications and Science'. Canadian Journal of Remote Sensing 40 (3): 192–212. https://doi.org/10.1080/07038992.2014.945827.

Wijaya, Putu Ananta, Muhammad Buce Saleh, and Tatang Tiryana. 2015. 'Spatial Model of Deforestation in Jambi Province for The Periode 1990–2011'. Jurnal Manajemen Hutan Tropika 21 (3): 128–37.

Xiangsheng, Kong, Qian Yonggang, and Zhang Anding. 2011. 'Haze and Cloud Cover Recognition and Removal for Serial Landsat Images'. Proceedings of SPIE - The International Society for Optical Engineering, November 2011. https://www.researchgate.net/publication/258547704_Haze_and_cloud_cover_recognition_and_removal_for_serial_Landsat_images.

8. Annex
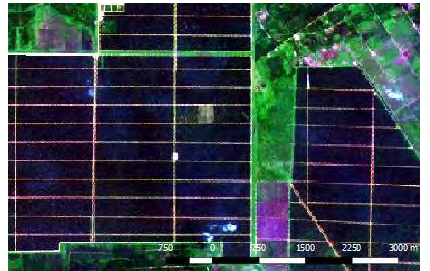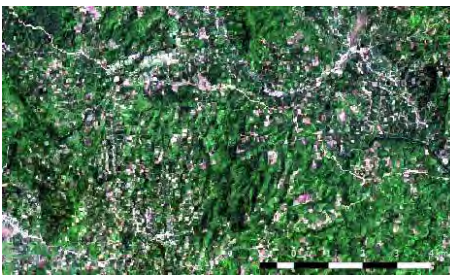
Annex 01

Table 12 Description and appearance in satellite image and in situ of different LC classes.

No	Macro-class	LC Class	Description	Land cover	Appearance in satellite image	Appearance in-situ
1	Forest	Primary / secondary dryland forest	Land cover with predominance of trees. Forest not permanently or seasonally flooded.	Trees adapted to dry conditions		
2	Forest	Primary / secondary swamp forest	Forest inundated with freshwater, permanently of seasonally. Near to rivers and lakes.	Trees adapted to wet conditions		
3	Forest	Primary / secondary mangrove forest	Forest with mangroves as main as tree species	Trees adapted to wet and salty conditions		

4	Forest	Plantation forest	Managed forest with trees of the same age	Mostly Acacia plantations		
5	Natural areas	Shrub/bushlands	Lands dominated by shrubs	Bushes and reminded trees in dry areas		
6	Natural areas	Swamp	Shrubs dominated in wetlands that occurs in temporally flooded areas	Bushes and reminded trees in dry areas		

7	Agriculture	Rubber	Agricultural land planted by rubber	Rubber plantations of different ages		
8	Agriculture	Oil palm	Agricultural land planted by oil palm	Oil palm plantations of different ages		
9	Agriculture	Dryland agriculture	Agricultural land planted by basic food crops	Cassava, tee, fruits among other crops		

10	Agriculture	Jungle rubber	Mixed agricultural lands cultivated within rubber plantations	Mixed rubber plantations		
11	Agriculture	Mixed garden	Agricultural crops and trees planted in family gardens	Family gardens		
12	Agriculture	Paddy field	Rice fields	Rice fields		

13	Others	Open/bare land	Lands with neither forests nor agricultural crops nor vegetation in general	Deforested areas, fallow lands and mining		
14	Water bodies	Water bodies	Water lands	Rivers, lakes and among other standing water		
15	Urban areas	Urban areas	Man-made lands	Cities and villages		

Annex 02:

Table 13 Visual interpretation - Classification key for classes allocated in red dot (see Figure 6) with number of classified points and proportions in percentage (p).

LC point - 1	LC point - 2	LC point - 3	Count	p (%)
Abiotic / non-vegetated	Artificial surface and constructions	Building / Roof	5	0.50
		Sealed Road	1	0.10
		Other-Artificial Surface	4	0.40
		blanks	1	0.10
	Nature Material Surface	Bare soils	30	2.97
		Unsealed roads	21	2.08
	blanks	-	1	0.10
Biotic / vegetation	Herbaceous Plants (grasses, forbs, crops)	-	84	8.33
	Woody Vegetation	Tree	359	35.58
		Palm	63	6.24
		Bush / shrub	72	7.14
		blanks	7	0.69
	blanks	-	81	8.03
Water	Lake	-	2	0.20
	River	-	9	0.89
Unclear	Clouds	-	10	0.99
	Image resolution	-	259	25.67
	TOTAL		1009	100

Annex 03:

Table 14 Supervised classification report, including pixel sums, proportion (%), and areas (m^2 and km^2).

|	Class	Pixel Sum	p (%)	Area (m^2)	Area (km^2)
1	Primary forest	55 218 224	25.12	12 343 638 866.70	12 343.64
2	Secondary forest	42 701 223	19.42	9 545 552 857.29	9 545.55
3	Plantation forest	11 547 220	5.25	2 581 298 406.01	2 581.30
4	Natural areas	16 389 440	7.46	3 663 742 038.99	3 663.74
5	Agriculture	17 109 764	7.78	3 824 765 314.98	3 824.77
6	Oil palm	32 663 311	14.86	7 301 649 454.97	7 301.65
7	Rubber	22 566 352	10.26	5 044 546 518.31	5 044.55
8	Water	2 599 694	1.18	581 142 991.85	581.14
9	Urban areas	2 434 459	1.11	544 205 889.92	544.21
10	Jungle rubber	16 612 787	7.56	3 713 669 662.70	3 713.67
	TOTAL	219 842 474	100	49 144 212 001.72	49 144.21

Annex 04:
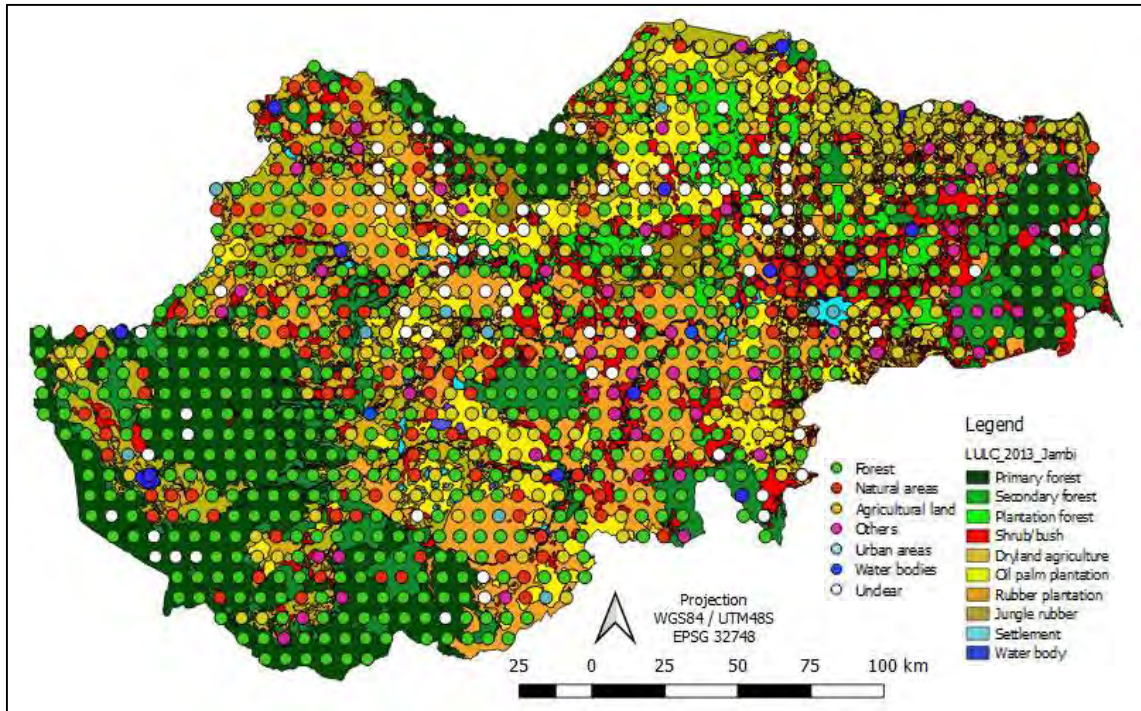
Figure 21 Overlapping map of 2013 classification and visual interpretation plots
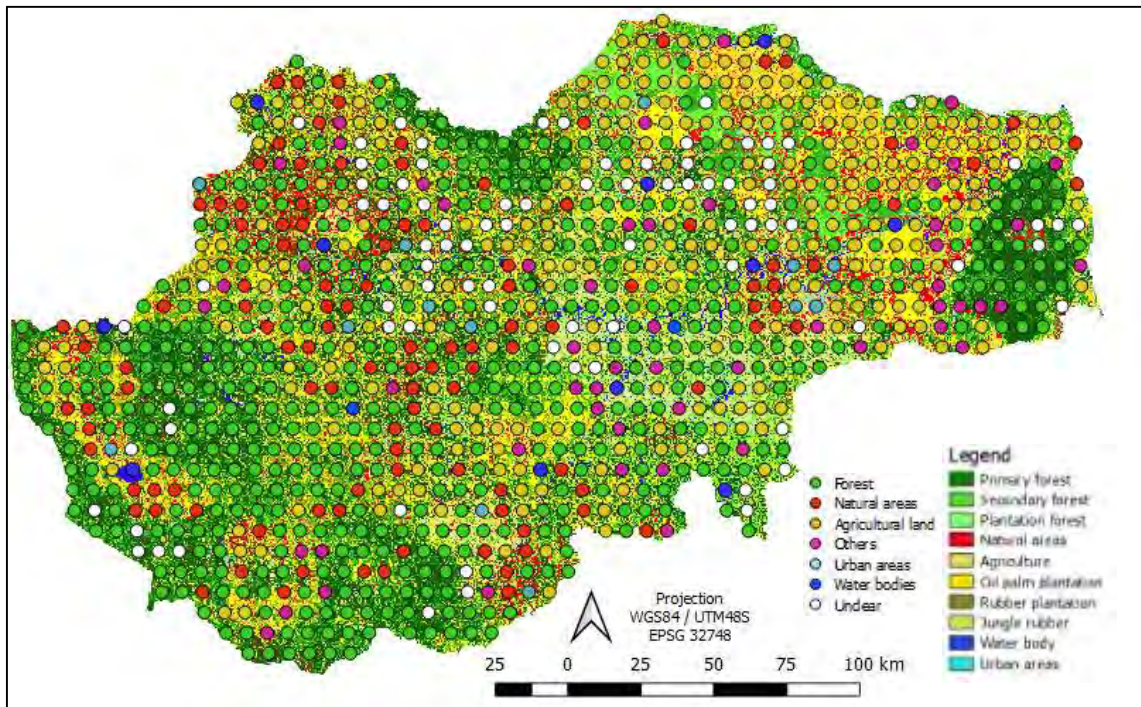
Annex 05:

Figure 22 Overlapping map of supervised classification and visual interpretation plots

Declaration of authorship

I hereby assure in accordance with § 7 (5) of the Master Examination Regulations of 23.09.2010 that I have written the present work independently and have not used any sources and aids other than those indicated.

December 20th, 2018

Rodrigo Paul Vera Ramirez